Overview of Probing Protein-Ligand Interactions Using NMR

Clémentine Aguirre,[1] Olivier Cala,[1] and Isabelle Krimm[1]

[1]Institut des Sciences Analytiques, UMR5280 CNRS, Ecole Nationale Supérieure de Lyon, Villeurbanne, France

Nuclear magnetic resonance (NMR) is a powerful technique for the study and characterization of protein-ligand interactions. In this unit we review both experiments where the NMR spectrum of the protein is observed (protein-observed NMR experiments) and those where the NMR spectra of the ligand is observed (ligand-observed NMR experiments) for the identification of binding partners, the measurement of protein-ligand affinity, the design of molecules that are active against biological targets such as proteins, and the assessment of the binding modes of the ligands. Ligand-observed methods discussed in this unit are Nuclear Overhauser Effect (NOE)—based approaches, with well-known experiments such as the Saturation Transfer Difference, Water-Ligand Observed via Gradient Spectroscopy (WaterLOGSY), and transferred—Nuclear Overhauser Effect Spectroscopy (tr-NOESY) experiments, and also the INPHARMA experiment. Regarding protein-observed experiments, this unit focuses on the use of chemical shift perturbations observed in protein-NMR spectra upon ligand binding. Also discussed is how these chemical shift perturbations can be used for the analysis of protein-ligand complexes, including fast structure determination when combined with docking. © 2015 by John Wiley & Sons, Inc.

Keywords: NMR • ligand • NOE • INPHARMA • WaterLOGSY • chemical shift perturbations • 3D structure

How to cite this article:
Aguirre, C., Cala, O., and Krimm, I. 2015. Overview of probing protein-ligand interactions using NMR. *Curr. Protoc. Protein Sci.* 81:17.18.1-17.18.24.
doi: 10.1002/0471140864.ps1718s81

INTRODUCTION

Molecular interactions are central for biological processes, all of which directly and indirectly depend on the interactions between molecules. For example, protein-protein and protein–small molecule interactions can regulate and modulate the function of proteins, and protein activity can be modified upon binding to ligands through mechanisms involving protein conformational changes. As a consequence, the analysis of protein-ligand interactions is particularly helpful for understanding the regulation of biological functions that occur in the cells. In this unit, we will only consider ligands to be low molecular weight organic compounds, of less than 1000 Da, that bind protein targets. Probing and analyzing protein-ligand interactions not only has a strong impact in basic research, but also in drug discovery, since the biological activity of drugs is related to their capability to bind proteins.

Protein-ligand interactions are characterized by several physico-chemical properties, such as the dissociation constant K_d, the thermodynamics with enthalpy ΔH and entropy ΔS contributions, and the kinetics (on and off rate constants), as well as the 3-D structures and the dynamics of the protein-ligand complex. A large variety of biophysical methods have been established for the analysis of protein-ligand interactions such as Surface Plasmon Resonance (SPR), Isothermal Titration Calorimetry (ITC), Fluorescence Polarization assay (FP), Fluorescence Resonance Energy Transfer (FRET), Enzyme-Linked

Current Protocols in Protein Science 17.18.1-17.18.24, August 2015
Published online August 2015 in Wiley Online Library (wileyonlinelibrary.com).
doi: 10.1002/0471140864.ps1718s81

Immunosorbent Assay (ELISA), Differential Scanning Fluorometry (DSF), MicroScale Thermophoresis (MST), and ElectroSpray Ionization Mass Spectrometry (ESI-MS). SPR and MST permit determination of kinetic parameters while ITC measures the thermodynamic parameters of interactions in solution. Computational calculations can also be used for virtual screening of compound libraries against a protein 3-D structure, to search ligands for a protein target, or propose 3-D models of protein-ligand complexes (docking calculations; Sousa et al., 2013). The experimental methods that allow determination of the 3-D structures of protein-ligand complexes at atomic resolution are X-ray crystallography and nuclear magnetic resonance (NMR) spectroscopy (Maurer, 2005; Mooij et al., 2006). None of these biophysical techniques are able to provide a full characterization of a protein-ligand complex. Rather, the best option is to use several biophysical techniques to identify ligands that bind protein receptors and then characterize the protein-ligand complexes.

Among biophysical methods, NMR spectroscopy is a well-known technique for probing protein-ligand interactions in a large range of affinities (nM to mM) (Carlomagno, 2012; Goldflam et al., 2012; Harner et al., 2013). A large diversity of NMR experiments exists, with very different experimental conditions both for the sample and the NMR parameters. Typically, the NMR experiments best suited for studying a particular protein-ligand interaction will depend on the molecular weight of the protein receptor, as well as the affinity and kinetics of the protein-ligand association/dissociation. The NMR methods are classically divided into two groups, the experiments where the NMR spectrum of the protein is observed (protein-observed NMR experiments) and those where the NMR spectra of the ligand is observed (ligand-observed NMR experiments). Protein-observed NMR experiments mostly rely on the analysis of chemical shift perturbations that occur on 2-D NMR spectra of ^{13}C- or ^{15}N-labeled protein samples upon ligand binding. These Chemical Shift Perturbations (CSPs) are used to distinguish specific from non-specific binding, to localize the binding site of ligands, and to measure protein-ligand dissociation constants. The 3-D structure of protein-ligand complexes can then be determined via heteronuclear experiments recorded on ^{13}C-, ^{15}N-, or ^{2}H-labeled protein samples. The structure resolution requires molecular dynamics calculations with experimental NMR restraints resulting from chemical shifts, scalar couplings, Nuclear Overhauser Effects (NOEs), paramagnetic interactions, or dipolar couplings (Breukels et al., 2011). These methods are limited in their routine use to proteins with low molecular weights (<30 kDa) to avoid large efforts in both labeling strategies and resonance assignment. The protein must be stable and soluble enough at a concentration of about 100 μM. When the X-ray apoprotein structure is available, the CSPs observed on protein NMR spectra, upon ligand binding can be used to assess the ligand binding mode [see Protein-observed NMR experiments: Chemical Shift Perturbations (CSPs) below].

In contrast to the protein-observed NMR experiments, the NMR parameters investigated in the ligand-observed NMR experiments are not chemical shifts, but rather NMR parameters that strongly depend on the molecular rotational correlation time τc, which is related to the molecular weight. Such parameters include transversal, longitudinal, and cross-relaxation rates. Ligand-based NMR experiments rely on the modification of such size-sensitive NMR parameters for the ligand, in the presence of a protein receptor (Ludwig and Guenther, 2009; Cala et al., 2014). Considering a protein-ligand complex with a weak to moderate affinity (typically 0.1 μM < K_d < mM), NMR parameters observed are a simple population-weighted average between the free and bound states. In contrast to protein-observed experiments, ligand-observed experiments are more sensitive with larger proteins, and require less protein without isotope labeling. Ligand-based methods can be used for the identification of binders and the measurement of protein-ligand affinities, and can provide pertinent structural information for the protein-ligand complexes as well.

The NMR role in drug discovery has become more pronounced in the last decade due to the success of the fragment-based approaches. Fragment-Based-Drug-Design (FBDD) is now recognized as an alternative approach to high-throughput screening for the drug discovery process (Erlanson, 2012), with the first drug approved in 2011 by the FDA, Zelboraf (vemurafenib), for forms of melanoma. The first step of the FBDD approach consists of identifying fragment-like compounds that bind the protein target through a minimal recognition motif. Fragments represent very small compounds (mol. wt. < 250 Da) with poor complexity; as a consequence they bind the proteins with weak affinities (usually K_d > 10 μM), but

exhibit high ligand efficiency (binding energy per heavy atom) due to high-quality interactions with the protein target (Murray et al., 2014). The second step for FBDD is the evolution of the initial fragment into an active potent molecule with nM activity. The fragment is successively modified through the addition of chemical groups, based on the structural information available for the protein-fragment complex. NMR plays an important role in FBDD, appearing as a robust screening approach for the identification and validation of fragment binders (Harner et al., 2013). NMR also plays also a less important role in the second step of the FBDD process, since X-ray crystallography is usually the method of choice for the elucidation of 3-D structures.

In this unit, we will focus on the NMR experiments that are experimentally easy to handle, and that can be used routinely for the characterization of protein-ligand interactions. We will first review ligand-observed NMR experiments that rely on NOE-based intermolecular magnetization transfer: transferred Nuclear Overhauser Effect Spectroscopy (NOESY), Saturation Transfer Difference (STD), and Water-Ligand Observed via Gradient Spectroscopy (WaterLOGSY) experiments. We will briefly recall the principles of the methods and describe different applications based on published examples. Secondly, we will discuss the use of protein-observed NMR experiments for detection of binders, the identification of the ligand-binding site, and the assessment of the binding modes of the ligands. In this section, we particularly emphasize the use of CSPs to generate protein-ligand complex structures.

LIGAND-OBSERVED NMR EXPERIMENTS

Transferred-NOESY, Inter-Ligand NOE (ILOE) and INPHARMA Experiments

Principle of the 2-D 1H-1H NOESY experiment

The ^{1}H-^{1}H NOESY experiment is a 2-D experiment that yields correlation signals caused by dipolar cross-relaxation between nuclei that are spatially close (less than 5 Å apart). Roughly, the peak intensity is related to the distance between the two protons. The maximum possible NOE depends on the molecular correlation time, which is related to the molecular weight and solvent viscosity: large molecules lead to large correlation times and produce large negative NOE peaks. By contrast, the NOE peak is positive for small molecules (mol. wt. < 500 Da) and goes through zero for medium-size molecules (mol. wt. range of 500 to 1000; Fig. 17.18.1). The NOE intensity reaches a maximum for a mixing-time value that

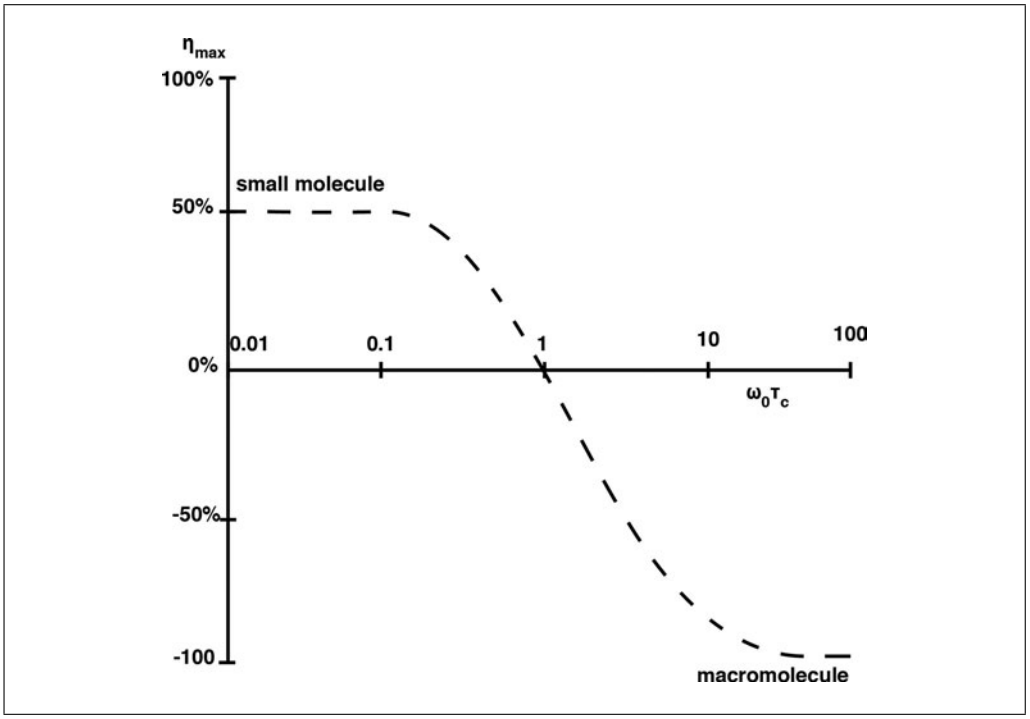

Figure 17.18.1 Dependence of the nuclear Overhauser enhancement η on the product $\omega_0\tau_c$, with ω_0: spectrometer frequency and τ_c: correlation time of the molecule.

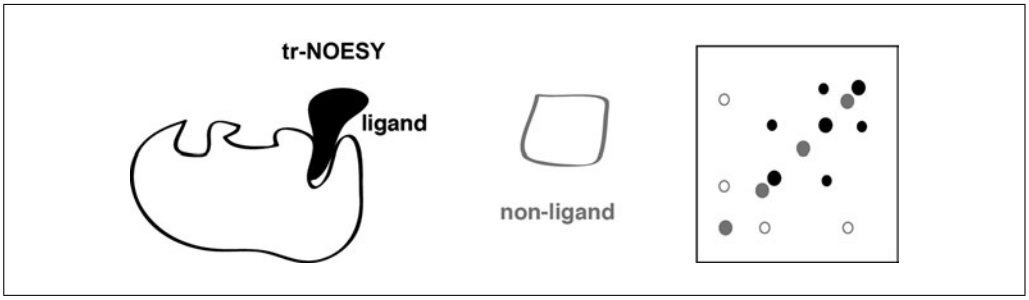

Figure 17.18.2 Transferred Nuclear Overhauser Effect Spectroscopy (tr-NOESY) experiment. The 2-D NOESY spectra observed for a ligand (black) and a non-ligand (gray) in the presence of a substoichiometric quantity of a protein target is shown. For the ligand, the tr-NOESY peaks are negative and large (symbolized by black filled circles), as the diagonal peaks. For the non-ligands, the negative diagonal peaks are shown in filled gray circles, while the tr-NOESY peaks are positive and weak (symbolized by empty gray circles). Selected intramolecular NOESY peaks are arbitrarily displayed.

depends on the molecular weight of the compound. Usually, large molecules build-up NOE quickly, while small molecules build up NOE more slowly. The maximum NOE is therefore shifted to shorter mixing times for large molecules. A shorter distance between protons will also lead to faster buildup of NOE, and a shift of the maximum to shorter mixing times.

The transferred-NOESY experiment

In the transferred-NOESY experiment, a NOESY spectrum is recorded on a sample of small-molecular-weight compounds in the presence of a substoichiometric amount of a protein receptor (Post, 2003; Ravindranathan et al., 2003). Transferred NOEs are observed in conditions of fast exchange, usually corresponding to dissociation constants within the μM to mM range. For small molecules that tumble rapidly in solution, the relaxation mechanisms lead to weak-positive NOESY peaks. By contrast, the ligands take a long correlation time when bound to the protein. In fast exchange conditions (dissociation rate constant, k_{off}, larger than the longitudinal relaxation rate, R1), this translates into strong negative—transferred NOEs in the 2-D NOESY spectrum of the free ligand. If a mixture of compounds is screened in presence of a protein receptor, the molecules that bind the protein will exhibit strong negative NOEs, whereas non-binders will show weak positive NOEs (see Fig. 17.18.2). The observation of transferred NOEs depends on the fraction of free and bound ligands, with the former and the latter giving rise to positive- and negative-NOE peaks, respectively.

Observation of ILOEs

When NOESY experiments are recorded in the presence of several ligands, for example when fragment libraries are screened using 2-D NOESY experiments, intermolecular ligand-ligand NOEs can be observed. A theoretical example is shown in Figure 17.18.3, with two ligands binding simultaneously in adjacent binding pockets of the protein, forming a ternary complex. ILOEs were reported for the first time for the complex formed by NAD^+ and lycolate in the presence of lactate dehydrogenase (Li et al., 1999). While ILOEs have been observed with other protein receptors (Chen et al., 2007; Rademacher et al., 2011), ILOE cross peaks are not detected for all ligand pairs, which might have been expected to produce such effects. These results are likely from insufficient formation of the ternary complex or from suboptima exchange kinetics.

Observation of INPHARMA peaks

Another type of inter-ligand NOESY peaks can be observed when two ligands bind competitively to the same protein-binding pocket with similar residence times. These NOESY cross peaks are called INPHARMA (Inter-ligand NOE for PHARmacophore MApping) NOEs and differ from the ILOE peaks, which are observed between two ligands binding simultaneously to adjacent binding pockets of the protein. The INPHARMA NOEs were described for the first time in 2005, with apothilone A and baccatin III binding to the tubulin (Sánchez-Pedregal et al., 2005). Similarly to the ILOEs, theoretical analysis shows that the observation of INPHARMA peaks strongly depends on kinetics (Orts et al., 2009).

INPHARMA and ILOE experiments are compared in Figure 17.18.3. In the INPHARMA experiment, ligand 1 binds the protein, and magnetization is transferred from

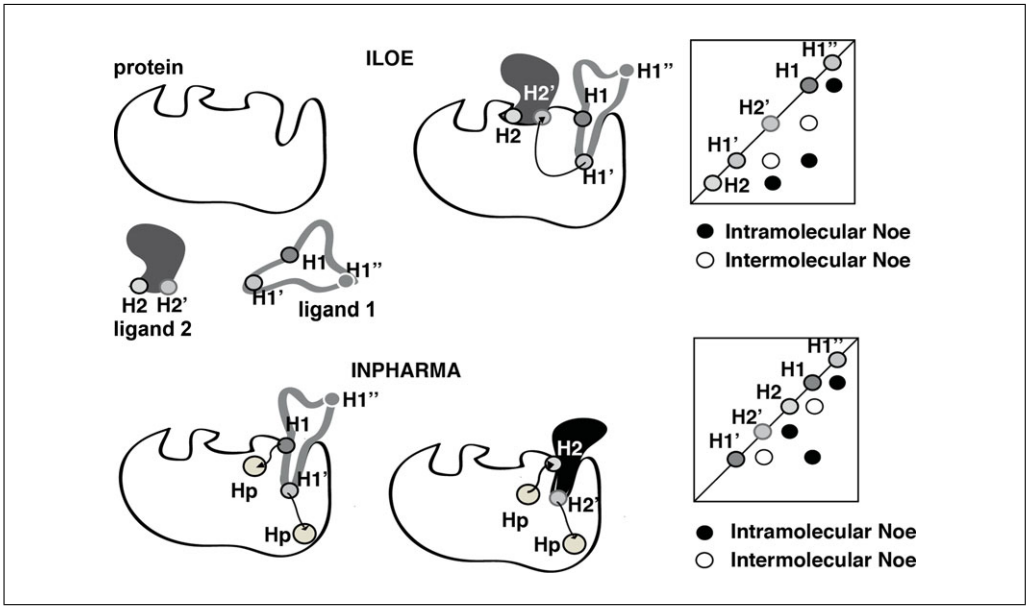

Figure 17.18.3 Inter-Ligand Nuclear Overhauser Effect (ILOE) and Inter-ligand Nuclear Overhauser Effect for PHARmacophore MApping (INPHARMA) experiments. For the ILOE experiment, a ternary complex is formed between the protein and two ligands. Inter-ligand NOEs are observed between protons of ligands 1 and 2 that are close (H1 and H2′, H1′ and H2′). For the INPHARMA experiment, two binary complexes are formed and an inter-ligand NOE is observed between protons of ligands 1 and 2 that have dipolar interactions with the same protein protons Hp (H1 and H2, H1′ and H2′). Theoretical NOESY spectra are displayed, showing the expected intermolecular ILOE or INPHARMA peaks. Not all the intramolecular NOESY peaks are displayed, and the symmetric peaks are not shown for clarity.

its proton H1 to the protein proton Hp. Subsequently, ligand 1 dissociates from the receptor, while ligand 2 binds into the same protein-binding site. The magnetization then transfers from the protein proton Hp to the proton H2 of ligand 2. This leads to an intermolecular NOE cross peak between H1 and H2. These inter-ligand NOE peaks can be used to define the relative binding mode of the two ligands in the same protein-binding pocket.

Experimental Conditions

NOESY mixing time

One major parameter of the NOESY experiment is the mixing time. Transferred-NOESY experiments typically require mixing times of 200 to 400 msec. For the observation of ILOE peaks between noncompetitive ligands, the mixing time is typically longer (600 to 800 msec), while the observation of INPHARMA peaks can be performed with lower mixing times (50 to 200 msec). As shown by theoretical studies, the optimal mixing time for INPHARMA depends on the correlation time and the internal dynamics of the complex (Orts et al., 2009). Roughly, the larger the complex, the shorter the mixing time for which the intensity of the INPHARMA has reached its maximal value.

Protein and ligand concentration

The ligand concentration for NOESY experiments typically ranges from 200 to 1000 μM. The protein concentration depends on its molecular weight, but remains in the low micromolar range. The optimum ligand to protein ratio varies from 10:1 for small proteins to > 100:1 for large proteins. For observing ILOE peaks, affinities and concentrations of the two ligands must be selected so that a substantial fraction of the receptor exists as a ternary complex. Usually, one compound is used as an ILOE probe. The ILOE probe should have a known binding mode with protons facing another binding site, to allow screening for compounds binding the adjacent pocket. Similarly, the affinities of competitive ligands need to be similar (the ratio of the K_d should be less than 10) to allow observation of INPHARMA NOEs (Orts et al., 2009).

Artifacts in transferred-NOESY experiments

Artifacts in transferred-NOESY experiments mainly originate from compound aggregation, nonspecific interactions, and spin

diffusion. It is therefore necessary to record the experiment in the absence of protein to ensure that the peaks observed are due to the protein binding and not to compound aggregation. Compound aggregation can be tested by WaterLOGSY experiments as well. While specific binding should generate NOE peaks with intensities related to the compound conformation upon binding, nonspecific interactions will translate into homogenous intensities for all NOE peaks observed for the molecules (Sledz et al., 2010). ILOEs can be observed in experiments performed with a perdeuterated protein, since the magnetization pathway does not include protein protons, but should be cancelled in the presence of a known competitor. By contrast, INPHARMA peaks are cancelled in the presence of a perdeuterated protein. When fragments are screened, some drawbacks of the transferred-NOESY experiments can be problematic, especially with aromatic compounds. In particular, zero-quantum peaks that occur between peaks that are J-coupled, such as ortho-protons on a benzene ring, are common artifacts in the NOESY spectra. In addition, the strong overlap in the 7- to 8-ppm region can make the observation of inter-ligand NOEs quite difficult. The transferred-NOESY experiment is therefore better suited to compounds that contain aliphatic groups, such as methyl and methylene groups. Another issue is the spin diffusion, usually observed with large protein receptors, which induces indirect transferred-NOEs (tr-NOEs), which may lead to interpretation errors for the calculation of the ligand bound conformation. To avoid this, short mixing times or transferred rotating-frame Overhauser effect spectroscopy (tr-ROESY) experiments can be used (Arepalli et al., 1995).

Applications of Transferred-NOESY Experiments

Fragment-based screening

The screening of fragments, which typically bind protein receptors with weak affinity in the μM to mM range, constitutes a standard application of the transferred-NOESY experiment (Meyer and Peters, 2003). One advantage of the method over the NOESY-based 1-D experiments, such as the STD and WaterLOGSY experiments, is the possibility to perform the experiment in very large mixtures (up to 96 compounds), which dramatically increases the throughput (Chen et al., 2007).

Conformation of the bound ligand

The transferred-NOESY experiment not only identifies ligands and screens ligand libraries, but also can provide structural information about the conformation of the bound ligand, the so-called bioactive conformation, through the analysis of the intra-molecular tr-NOEs (Post, 2003; Ravindranathan et al., 2003). Importantly, this does not necessitate the knowledge of the protein 3-D structure. A simple procedure consists of using the NOE cross-peak intensity as a method of quantifying distances. The method called Isolated Spin Pair Approximation allows for distance determination, by comparing the relative intensity of the NOE between a spin pair of known distance to that of a spin pair of unknown distance. Bound ligand structures are then generated using molecular dynamics—minimization procedures. Nevertheless, precautions are usually required to prevent issues due to spin diffusion. One approach is based on the comparison of experimental NOEs with back-calculated NOEs based on protein-ligand models using Complete Relaxation and Conformational Exchange MAtrix (CORCEMA; Moseley et al., 1995). CORCEMA explicitly includes all relevant protons involved in the interaction and can include the effect of dynamic movements within the complex. For a comprehensive review of the method, refer to the research of Jayalakshmi and Krishna (2002).

Identification of the ligand-binding site using INPHARMA

INPHARMA peaks observed for two compounds that bind the same protein pocket can be used to identify the binding site of a ligand in the presence a reference compound with a known binding site. For example, INPHARMA experiments have been performed with the glycogen phosphorylase (GP) enzyme for fragments derived from a simple deconstruction of GP inhibitors (Krimm, 2012). The GP protein, a therapeutic target in type 2 diabetes, has four distinct binding sites: the active site, the inhibitor site, the allosteric site, and the so-called new allosteric site. NOESY experiments performed for six fragments in the presence of two reference molecules have shown that INPHARMA experiments are useful in FBDD to identify the binding site of fragments. The combination of INPHARMA and STD experiments allows for distinguishing between competitors, ligands that bind other protein binding sites, and non-specific binders.

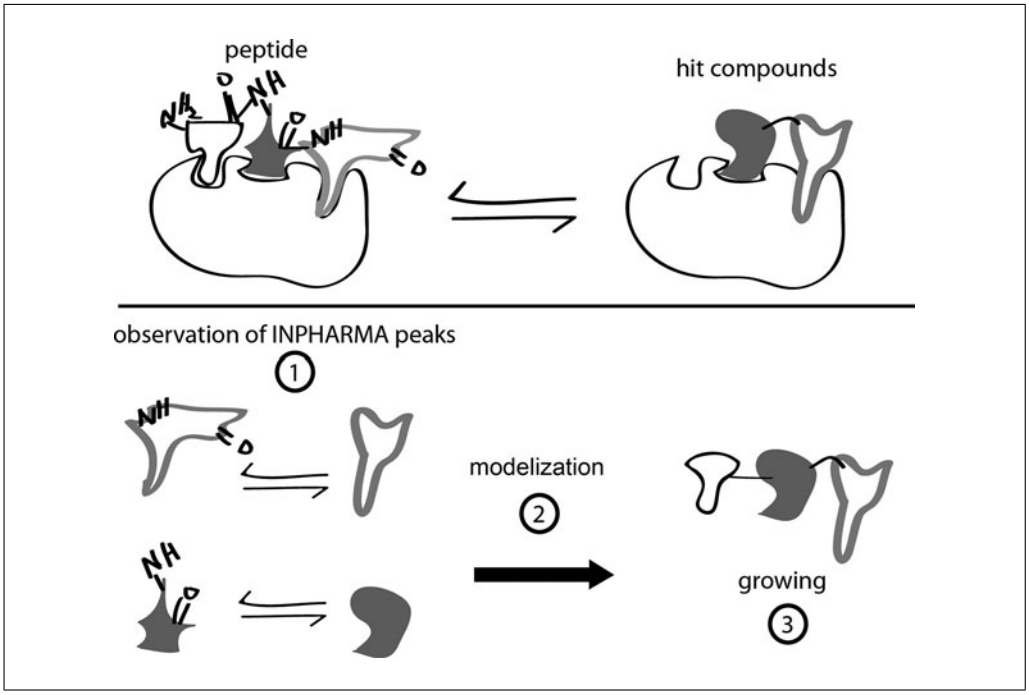

Figure 17.18.4 Inter-ligand Nuclear Overhauser Effect for PHARmacophore MApping (INPHARMA)-based design of protein inhibitors using known protein-peptide interactions. The interactions of the protein target and a peptide are compared to the interactions of the protein with a hit compound using INPHARMA experiments. INPHARMA peaks and modelization allow the identification of the peptide region that can be added to the hit compound, to obtain a lead molecule with an improved affinity.

Assessment of the ligand-binding mode using INPHARMA

The INPHARMA cross peaks observed between the protons of two competitive ligands can be used to define a relative orientation of the ligands in the protein-binding pocket. To generate precise structural information, a full relaxation matrix approach is required to interpret the NOESY experiments recorded at different mixing times (Reese et al., 2007).

Nevertheless, a qualitative analysis of INPHARMA data can also provide valuable structural information for structure-based drug design, as well as in the FBDD process (Bartoschek et al., 2010; Krimm, 2012).

Design of protein inhibitors using INPHARMA

The INPHARMA experiment can be used to compare the binding modes of a competitive peptide ligand and a synthesized inhibitor. The main idea is to discriminate overlapping and non-overlapping peptide-compound pharmacophores, using the data inferred from the INPHARMA cross peaks observed between the peptide and the ligand. Then, non-overlapping regions of the peptide can be added to the inhibitor, to design a modified inhibitor and improve the interactions of the latter, with the protein receptor (Fig. 17.18.4; Ono et al., 2014). The approach has been applied to the design of an inhibitor derived from the losartan molecule, for the inhibition of platelet receptor glycoprotein VI collagen interaction. A 12-amino acid peptide, pep-10 L which inhibits the glycoprotein VI—collagen interaction with a K_d of 5.7 10^{-5} M, was used. INPHARMA experiments with 1.4 mM losartan, 0.9 mM pep-10 L and 0.025 mM protein were conducted at various mixing times (60, 100, 200, and 300 msec) in D_2O. Regions of the peptide and the losartan molecules that interact similarly with the protein were clearly identified. An important region of the peptide for protein binding (including a phenylalanine residue) was shown not to overlap with losartan. This region constitutes, therefore, an additional interaction site that could be added to the losartan compound. The INPHARMA data were used to estimate the distance between atoms of losartan and the new interaction site. New compounds were designed and tested for the inhibition of the glycoprotein VI—collagen interaction. This strategy can be generalized for the design of protein inhibitors when a protein-peptide interaction is known, as illustrated in Figure 17.18.4.

Design of protein inhibitors using ILOEs

The first application of ILOEs in drug discovery was reported by the group of Pellecchia. The ILOE approach was successfully applied for the rational design of ligands that bind the Bid, Bcl-xL, and Mcl-1 proteins, which are all key members of the anti-apoptotic Bcl-2 family proteins, as well as isoform-specific inhibitors of the mitogen-activated protein kinase p38alpha (Becattini et al., 2006; Chen et al., 2007; Rega et al., 2011). Using a library of fragments, ILOE-based screening led to the identification of ligand pairs that bind in proximal sites within the co-factor binding pocket of human thymidylate synthase (Begley et al., 2010). Very recently, the method was applied for the identification of adjacent site ligands to the fucose binding site norovirus Virus-Like Particles (Rademacher et al., 2011). The method is nevertheless somewhat limited because the ILOE signals are often very weak due to insufficient saturation of the binding sites.

Saturation Transfer Difference (STD) Experiment

Principle of the experiment

Like the transferred-NOESY experiments, the STD experiment relies on magnetization exchange from the protein-bound state to the free state of the ligand. The method consists of applying a radiofrequency irradiation to selectively saturate the protein NMR signals without perturbing the resonances of the small molecules. The saturation then spreads via the NOE and spin diffusion. All the protein resonances are therefore saturated, which induces a strong attenuation of the NMR spectrum. When a molecule binds to the protein surface, the saturation of the protein protons is transferred to the molecule via spin diffusion through intermolecular NOEs. As illustrated in Figure 17.18.5, the STD experiment involves the subtraction of two 1-D spectra, one with saturation of a resonance of the macromolecule (STD-on), and another without saturation of the protein resonances (STD-off). In the case of on-resonance saturation of the protein protons (STD-on), the signals of the compounds that bind the protein will be saturated (and thus attenuated). By subtracting the spectrum corresponding to the off-resonance saturation of the receptor (STD-off), only the signals of the binders are observed, while the signals of the protein and non-binders are subtracted (Fig. 17.18.5).

Like the NOESY-based approaches, the STD experiment has several advantages for the identification of small molecules binding to a macromolecule: (1) it can be run without labeling or immobilization of either the ligand or the receptor, (2) the size of the receptor is not a limiting factor, (3) it can be used as an NMR screening method to pinpoint binders in a mixture (Mayer and Meyer, 1999), (4) it can be used to define the so called binding epitope, that is, the portions of the ligand with the closest contact with the receptor (Mayer and Meyer, 1999), and (5) it can even supply information about the conformation of the bound ligand in the complex if strategically combined with modeling (Siebert et al., 2002; DiMicco and Zaretsky, 2005; Yuan et al., 2005).

Experimental conditions

Saturation Transferred Difference spectra are performed with a large excess of ligand, corresponding to a protein-to-ligand ratio of 1:100 for medium-size proteins to 1:1000 for large proteins (mol. wt. > 80 kDa). The protein concentration typically ranges from 0.1 nM to 10 μM. The minimal molecular weight of the protein receptor is around 15 kDa. Saturation times are usually 1 to 2 sec. The selective saturation is placed in a region of the proton spectrum where signals of the protein, but not the ligands, are observed. This region is typically around 0 ppm, from -0.5 to 1 ppm. When ligands have no aromatic groups, the saturation frequency can be set in the region of the protein amide protons (8 ppm). The STD-off spectrum is obtained with a selective saturation, in an empty region of the spectrum, around 15 to 30 ppm. The saturation is usually obtained with a train of low power selective Gaussian pulses of 50 msec, separated by a 0.1 msec delay. In case of strong overlap of the compound resonances, in particular with carbohydrate compounds, the STD experiment can be combined with other pulse sequences such as correlation spectroscopy (COSY), total correlation spectroscopy (TOCSY), and heteronuclear multiple-bond correlation spectroscopy (HSQC) to resolve assignment ambiguities (Räuber and Berger, 2010). For similar purposes, ^{13}C and ^{19}F isotope edited STD experiments, which do not require sample labeling, have been proposed (Nagaraja, 2006; Räuber and Berger, 2010).

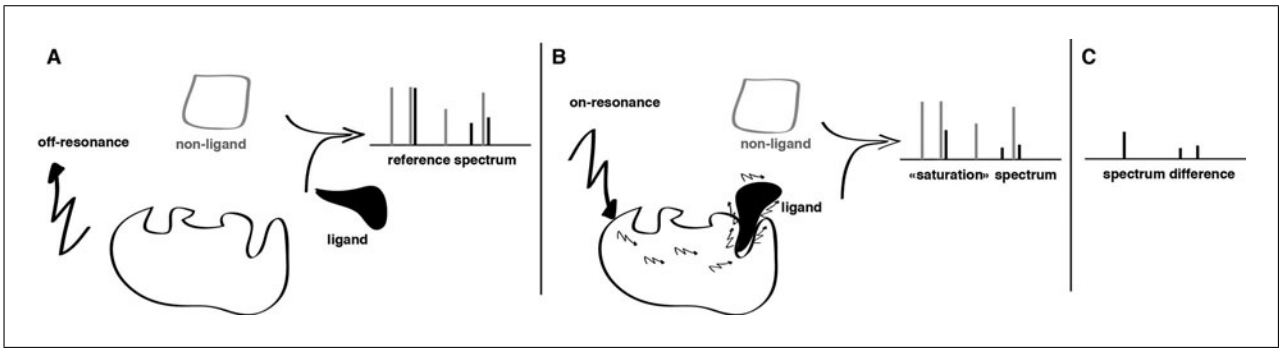

Figure 17.18.5 Principle of the Saturation Transfer Difference (STD) experiment. The principles of (**A**) the off-resonance saturation, (**B**) the on-resonance selective saturation of protein protons, and (**C**) the resulting STD spectrum are shown. Only the resonances of the ligand are visible in the STD spectrum. On-resonance saturation typically saturates the methyl groups of the protein.

Applications of the STD experiment

Detection of interactions and library screening

The STD experiment is a popular and highly versatile screening method for the identification of protein-ligand interactions over an extraordinarily broad affinity range (Mayer and Meyer, 1999; Meyer and Peters, 2003; Bhunia et al., 2012; Wagstaff et al., 2013) and is widely used for fragment-based screening (Campos-Olivas, 2011). Other specific applications include the detection and characterization of ligand binding to viruses (Benie et al., 2003; Rademacher et al., 2008) and membrane proteins integrated in liposomes (Meinecke and Meyer, 2001). Protein-ligand interactions can be observed directly in living cells with the saturation transfer double difference (STDD) method, where a second STD experiment is performed with the same sample but in the absence of the ligand, to remove the STD signals due to the other recognition events in the complex cellular sample (Claasen et al., 2005; Mari et al., 2005). The STDD method was first reported in 2005 with the observation of a cyclic peptide ligand binding to the receptor integrin αIIbβ3 present in liposomes (Claasen et al., 2005). More recently, STD was used to screen marine natural products against cannabinoid G-protein-coupled receptors CB1 and CB2 (Pereira et al., 2009).

It is also possible to study high-affinity ligands (K_d < 10 nM) by STD, by competition STD experiments. A reference molecule, with a moderate affinity (100 nM < K_d < 100 μM), must be available (Wang et al., 2004). For example, competition STD experiments have been used for the identification of protein kinase inhibitors. The ATP molecule, which binds to kinases with K_d in the μM range, is used as a reference molecule to find ATP competitors (McCoy et al., 2005). Another application of the STD experiment is the analysis of allosteric enzymes: it was recently shown that STD experiments performed on protein-fragment complexes can reveal the synergetic binding interactions for the allosteric proteins (Krimm et al., 2012).

Epitope mapping

STD experiments not only can be used qualitatively to identify binders, but STD can also give quantitative information about the binding, through the analysis of the STD intensities. Comparing the relative percentages of saturation received by the different ligand protons leads to the identification of the epitope, the chemical moieties of the ligand molecule that are key for the molecular recognition. The epitope mapping is obtained by normalizing the measured STD intensities (Equation 17.18.1) against the most intense STD signal that is assigned to 100%. The stronger the intensity of the STD signal, the shorter the corresponding protein-ligand proton-proton distance (Mayer and Meyer, 2001).

$$\mathrm{STD} = \frac{I_{\mathrm{STD}}}{I_0} = \frac{(I_0 - I_{\mathrm{SAT}})}{I_0}$$

Equation 17.18.1

I_{STD} is the intensity of the STD signals measured on the STD spectrum, and I_0 is the intensity of the STD signals measured on the off-resonance STD spectrum. Artifacts in the epitope definition can be due to the different relaxation rates R1 of the ligand protons. Protons with slower R1 relaxation display artificially increased STD signals. To overcome this issue, it has been proposed to derive STD intensities close to zero saturation time, by fitting the experimental buildup curves to the mono

exponential function (Mayer and James, 2004; Angulo and Nieto, 2011; Equation 17.18.2):

$$\mathrm{STD_{test}} = \mathrm{STD_{max}}(1 - \exp(-k_{sat}t_{sat}))$$

Equation 17.18.2

where $\mathrm{STD_{test}}$ is the observed STD intensity, $\mathrm{STD_{max}}$ is the asymptotic maximum of the buildup curve, and t_{sat} is the saturation time. k_{sat} and $\mathrm{STD_{max}}$ are derived by least-squares fitting. The initial slope of the curve is obtained as shown in Equation 17.18.3:

$$\mathrm{STD_0} \equiv \frac{d\mathrm{STD}}{dt}|_{t-0} = \mathrm{STD_{max}}k_{\mathrm{sat}}$$

Equation 17.18.3

The $\mathrm{STD_0}$ values are used to define the epitope mapping, which in these conditions is independent of the relaxation R1 of the ligand protons.

Affinity measurement

Mayer and Meyer (2001) proposed to calculate the STD amplification factor ($\mathrm{STD_{AF}}$), which is the intensity of an STD signal corrected by the excess of ligand, to obtain STD-derived values that are a function of the fraction of the bound protein (Equation 17.18.4):

$$\mathrm{STD_{AF}} = \mathrm{STD}^{[\mathrm{L_T}]}_{[\mathrm{P_T}]}$$

Equation 17.18.4

Although there is no simple correlation between $\mathrm{STD_{AF}}$ and the dissociation constant K_d, $\mathrm{STD_{AF}}$ values are used to determine affinities of the protein-ligand complexes. The amplification factor $\mathrm{STD_{AF}}$ depends on the fraction of bound protein f_{complex} (Equation 17.18.5):

$$f_{\mathrm{complex}} = \frac{[\mathrm{L}]}{K_\mathrm{d} + [\mathrm{L}]}$$

Equation 17.18.5

In conditions of ligand excess, [L] can be approximated to $[\mathrm{L_T}]$ (Equation 17.18.6), so that:

$$f_{\mathrm{complex}} = \frac{[\mathrm{L_T}]}{K_\mathrm{d} + [\mathrm{L_T}]}$$

Equation 17.18.6

The dissociation constant K_d is then determined by plotting the normalized $\mathrm{STD_{AF}}$ values at increasing total ligand concentrations. As was well documented in two major references (Angulo et al., 2010; Angulo and Nieto, 2011), errors in the K_d measurements are larger for ligand protons exhibiting large STD intensities and for larger protein concentrations. In general, the K_d values obtained depend on the STD signals chosen to build the curves, and also on the saturation time and the protein/ligand ratio. These errors were explained by the fast ligand rebinding and the accumulation of saturated ligand in solution (Angulo et al., 2010). As for the epitope mapping effect, such effects are minimized with a saturation time close to zero. Therefore, it has been proposed to determine the initial slopes of the buildup curves of $\mathrm{STD_{AF}}$ values with the saturation time. This requires recording a saturation time—dependent $\mathrm{STD_{AF}}$ buildup curve for each ligand concentration, to extract the initial slope $\mathrm{STD_{AF0}}$. The $\mathrm{STD_{AF0}}$ values are then plotted for each ligand concentration and the K_d is obtained by fitting it to the Langmuir equation (Angulo et al., 2010; Angulo and Nieto, 2011; Szczepina et al., 2011; Basilio et al., 2012). This method should enable the K_d measurement for aromatic ligands, where the very slow relaxing protons give bad results (Angulo and Nieto, 2011; Szczepina et al., 2011).

It is also possible to achieve K_d measurements if STD signals are measured in the presence of an inhibitor (Szczepina et al., 2009; Angulo et al., 2010). In the presence of a saturating amount of the inhibitor, STD signals correspond to nonspecific binding. The STD signals due to specific binding are obtained by the difference of the two spectra.

Quantitative STD using CORCEMA

The CORCEMA method, first developed for the analysis of NOEs peaks, has been modified to enable the prediction of STD intensities using a 3-D structure of a protein-ligand complex (Jayalakshmi and Krishna, 2002). Conditions of the method's application are that the dissociation constant K_d, the dissociation rate constant k_{off}, the rotational correlation time τc of the receptor, and the ligand are known. The comparison of the STD buildup curves and the predicted STD are done using the so-called R-NOE factor that calculates the agreement between the experimental and calculated STD intensities.

This procedure can also be used for the prediction of the initial STD buildup slopes

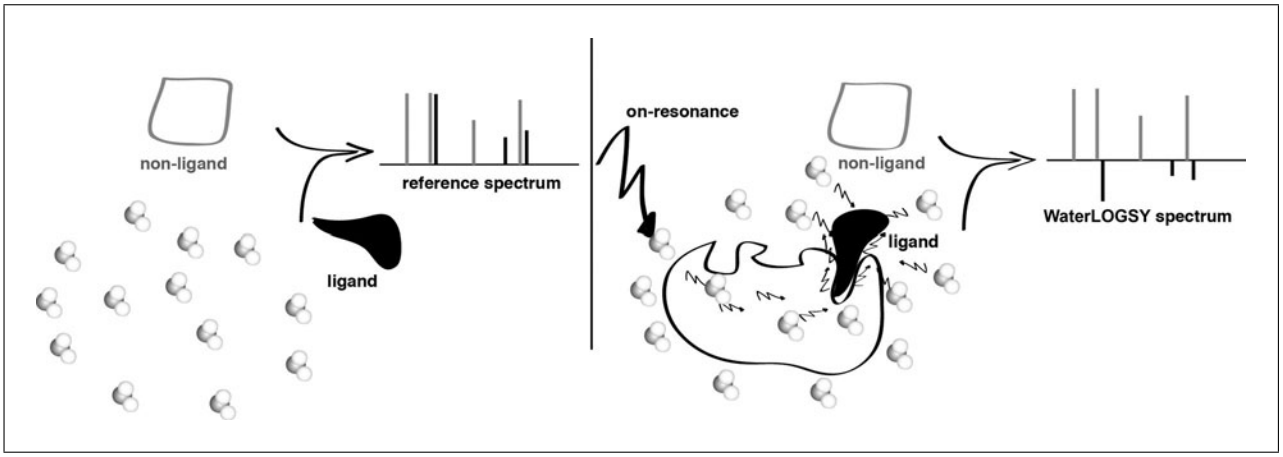

Figure 17.18.6 Principle of the Water-Ligand Observed via Gradient Spectroscopy (WaterLOGSY) experiment. A reference WaterLOGSY spectrum of the molecules (non-ligand in gray and ligand in black) must be recorded in the absence of the protein receptor (left). For the WaterLOGSY spectrum in the presence of the protein, the ligand and the non-ligand display peaks with opposite signs.

around $t_{sat} = 0$ for different binding modes of a ligand, to demonstrate whether the ligand exhibits multiple binding modes, and to elucidate the different binding modes of a protein-ligand complex (Angulo and Nieto, 2011).

WaterLOGSY Experiment

Principle of the experiment

As with the STD experiment, WaterLOGSY (Water-Ligand Observed via Gradient Spectroscopy) implies transfer magnetization via intermolecular NOE and spin diffusion (Dalvit et al., 2000a, 2001, 2002). Here, water molecules are involved in the transfer pathway. The bulk water magnetization is excited and transferred during the NOESY mixing time to the bound ligand via different mechanisms (Fig. 17.18.6): (1) direct transfer from water molecules immobilized in the protein binding site (water residence times > nsec) (2) chemical exchange between excited water and protein labile protons (amide, hydroxyl, amino) and propagation of the inverted magnetization into the ligand by intermolecular dipole-dipole cross-relaxation as well as spin diffusion, via the protein-ligand complex, and (3) transfer from the water molecules found in the protein cavities via the protein-ligand complex.

Independent of the number of hydrogen bonds that are formed, the residence times of water range between a few nsec to a few hundred μsec. For residence times longer than 300 psec, the protein-water NOEs are negative, with a large magnitude (Dalvit et al., 1999, 2000a). The molecules that interact with water via water-ligand-protein or protein-ligand complexes exhibit, therefore, a negative NOE with water, while the molecules that do not bind the protein will have weak and positive intermolecular NOEs with water. Therefore, binders and nonbinders can be discriminated in a WaterLOGSY spectrum, as they display opposite signs for their corresponding peaks. Another mechanism involves the magnetization transfer from the water to labile protons of the small molecules by chemical exchange. In this case, the transfer keeps the inverted sign of the magnetization. Such protons will therefore behave as false positive (WaterLOGSY peaks in the same sign as the WaterLOGSY peaks of binders) for both binders and nonbinders. It is thus important to record a WaterLOGSY spectrum of the molecule in the absence of the protein receptor to correct this effect (Dalvit et al., 2000a, 2000b, 2001, 2002).

Experimental conditions

As with the STD experiment, WaterLOGSY spectra are recorded with a substoichiometric quantity of the protein receptor. Typically, protein concentration is in the low μM range. Dalvit et al. (2001) report the application of the method with protein concentrations as low as a few hundred nM. However, while large ligand/protein ratios are used for the STD experiment, large ligand/protein ratios should be avoided for WaterLOGSY. The WaterLOGSY spectra reflect both the free and bound states of the ligand, therefore, the ratio should not exceed 100:1. Ligand concentration in WaterLOGSY experiments can be lower than in STD experiments, and classically ranges from 40 μM to 1 mM. WaterLOGSY experiments should therefore be preferred when ligands are not highly

soluble. Regarding the mixing time parameter, it typically varies from 1 to 3 sec in the literature.

Applications of the WaterLOGSY experiment

Screening and affinity measurement

The standard application of the WaterLOGSY experiment is the screening of fragment libraries. Using competition experiments, the method is also used to identify the ligand-binding site in the presence of a competitor (Dalvit et al., 2002). The determination of dissociation constants can be done by competition and titration experiments (Dalvit et al., 2001, 2002). Similarly to the STD experiments, intensities of WaterLOGSY signals can be used to rank the hits identified from the same experiments (Barelier et al., 2010).

Epitope mapping and water accessibility in protein-ligand complexes

It was recently proposed to use WaterLOGSY experiments for the discrimination of buried protons from solvent-exposed protons of ligands bound to protein receptors (Ludwig et al., 2008; Ludwig and Guenther, 2009). The method is called Solvent Accessibility, Ligand binding and Mapping of ligand Orientation by NMR spectroscopy (SALMON). Theoretically, the spin diffusion process has to be minimized, which is practically done by increasing the temperature of the experiment or reducing the NOESY mixing time (125 msec). Identification of solvent-accessible regions of ligands bound to proteins can then be used to orient the ligand into the binding pocket.

PROTEIN-OBSERVED NMR EXPERIMENTS: CHEMICAL SHIFT PERTURBATIONS (CSPs)

Principle of Protein-Observed NMR

Protein-observed NMR experiments rely on comparison of NMR parameters of the free and bound states of the macromolecule. The changes in the chemical shifts of the protein upon ligand binding, which are typically observed in 2-D HSQC or HMQC spectra, are used for: (1) the detection of ligand binding (2) the identification of the binding sites of the ligands, or (3) the determination of the atomic-resolution molecular structures of protein-ligand complexes. While ligand-observed NMR experiments require weak to moderate protein-ligand affinities for the binding to be directly observed, protein-observed NMR experiments can detect binding events for very weak (mM) or very strong (nM) ligands.

Exchange regime and chemical shift

The simplest kinetic scheme for a ligand L binding to a protein P is described as a second order exchange process (Equation 17.18.7):

$$P + L \leftrightarrow PL$$

Equation 17.18.7

with

$$K_d = \frac{[PL]}{[P][L]} = \frac{k_{off}}{k_{on}}$$

Equation 17.18.8

where k_{on} is the rate constant for the forward reaction (association) and k_{off} is the rate constant for the backward reaction (dissociation; Equation 17.18.8).

The effect of the exchange process on the NMR spectrum depends upon the rate constants relative to the magnitude of the change in the NMR parameters. When the exchange rate is fast on the chemical shift time scale, i.e., when k_{off} is much greater than the chemical shift difference, then the signals will move smoothly from their position in the free spectrum to those in the bound spectrum, with the frequency of the signal at any titration point being the weighted average of free and bound chemical shifts (Fig. 17.18.7A).

When the exchange rate is slow on the chemical shift time scale, or in other words when k_{off} is significantly slower than the difference in Hz between the chemical shifts of free and bound protein forms, then, as the ligand is titrated in, the free signal gradually disappears and the bound signal appears, as the intensities of the two peaks reflect the concentrations of the free and bound protein (Fig. 17.18.7B).

In case of fast exchange regime, multiple binding modes can be detected as illustrated in Figure 17.18.7A. For a single binding mode, the peaks move in a straight line with increasing concentrations of ligand. By contrast, multiple binding sites or modes will generate curved plots, because the secondary interactions will have different effects on the chemical shifts than the primary interaction.

The exchange regime for a protein-ligand system under investigation is determined by

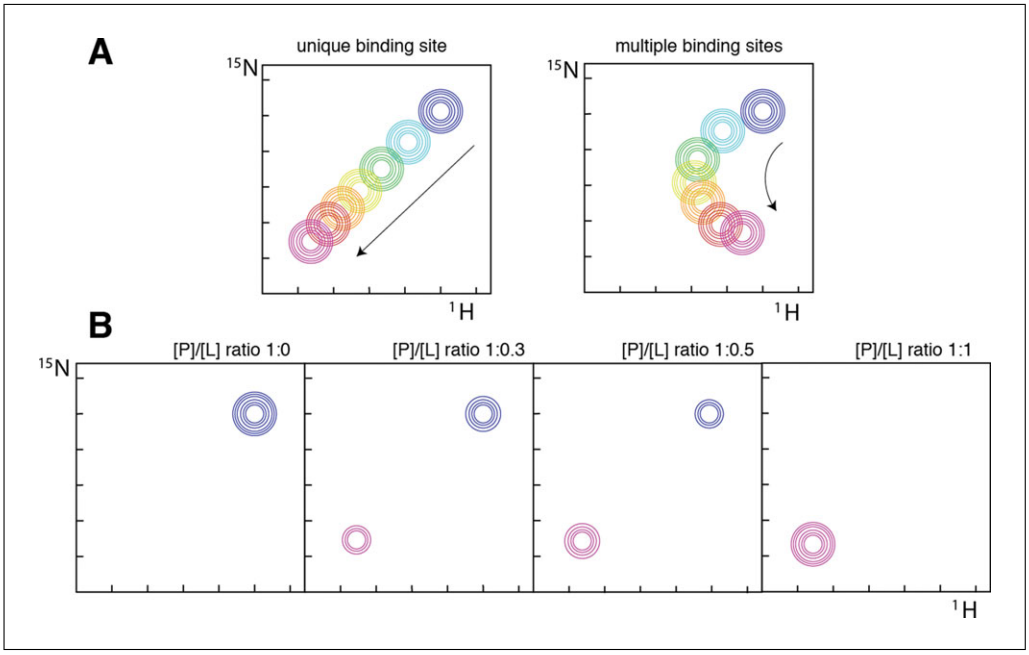

Figure 17.18.7 Protein nuclear magnetic resonance NMR spectra observed upon ligand binding in the case of fast (A) and slow (B) exchange. (**A**) Protein spectra observed upon ligand binding in case of (left) a single binding site or (right) multiple binding sites. Theoretical spectra are superimposed for seven different ligand concentrations increasing from blue to pink peaks. (**B**) In the case of slow exchange, protein spectra are displayed for three increasing ligand concentrations from the left to the right, showing the peak of the bound protein that appears (pink), while the peak of the free protein disappears (blue).

monitoring the changes in the protein NMR spectrum during a titration with ligand. This is usually realized by recording 2-D HSQC or HMQC NMR spectra with increasing ligand concentrations. As the concentration of ligand is increased, changes in the spectrum provide information on the chemical exchange regime (Fig. 17.18.7). The exchange rate depends on the spectrometer field, and fast and slow exchange behavior can also be observed for the same protein-ligand complex on the same NMR spectrum for different protein signals.

CSP Measurement

The Chemical Shift Perturbation (CSP) is typically measured on 2-D protein spectra and corresponds to the difference between the bound and free protein chemical shifts, measured on ^{1}H, ^{15}N, or ^{13}C resonances (Equation 17.18.9):

$$CSP = CSP_{bound} - CSP_{free}$$

Equation 17.18.9

Because the CSPs are measured on several resonances, such as ^{1}H, ^{15}N, or ^{13}C resonances, one usually calculates a combined CSP value (Equation 17.18.10):

$$CSP_{combined} = \sqrt{\frac{1}{N}\sum_{i=1}^{N}(\alpha_i.CSP_i)^2}$$

Equation 17.18.10

with i the nucleus and αi the corresponding scaling factor for the CSP value, and N the total number of nuclei. The values of the scaling factor α have been largely tested and documented in the literature (Williamson, 2013). Consider that α for ^{1}H is 1, α for ^{15}N usually ranges from 0.1 to 0.45, and the optimal value for ^{13}C is 0.3.

Experimental Conditions

Protein-observed NMR experiments require isotropically enriched protein samples. This is achieved by protein production with $^{15}NH_4Cl$ and ^{13}C glucose in the production medium. When the protein size is larger than 30 kDa, it is usually necessary to prepare deuterated samples. The pH must be carefully checked upon ligand addition, since small pH variations can induce chemical shift changes and complicate the CSP analysis. Temperature must also be identical for all experiments. By

contrast with NOESY-based ligand-observed NMR experiments that are more efficient at low temperature, HSQC or HMQC experiments should be conducted at higher temperature (25° to 35°C). The protein concentration for such experiments is relatively large and typically ranges from 50 to 500 μM.

Applications

Affinity measurement

The affinity of a protein-ligand complex can be determined by monitoring the changes in protein chemical shifts upon ligand titration. The protein-ligand complex must be in fast exchange on the NMR time scale (as described above). The experimental NMR signal S observed is the weighted average between the bound (S_{bound}) and the free (S_{free}) protein NMR signal (Equation 17.18.11):

$$S_{NMR} = x_{free} S_{free} + (1 - x_{free}) S_{bound}$$

Equation 17.18.11

with x_{free} corresponding to the free protein fraction in solution.

If one assumes a protein target P with one unique ligand L binding site, the experimental CSPs are related to the complex dissociation constant K_d as shown in Equation 17.18.12):

$$CSP = CSP_{max} \frac{[L_0] + [P_0] + K_d - \sqrt{([L_0] + [P_0] + K_d)^2 - 4[L_0][P_0]}}{2[L_0]}$$

Equation 17.18.12

where $[L_0]$ and $[P_0]$ are the ligand and protein concentrations and CSP_{max} is the maximum chemical shift change upon saturation. K_d values are determined by fitting the $[L_0]/[P_0]$ values to the CSP values using Equation (17.18.12). The shapes of the titration curves strongly depend on the complex affinity, as illustrated in Figure 17.18.8. The ideal case is represented by the curve plotted for $K_d = 0.1$ mM and a protein concentration of 0.1 mM. The ligand and protein concentrations must therefore be carefully chosen to obtain a curvature as optimal as possible. A detailed analysis has shown that the optimal value for the protein concentration is close to 0.5 K_d (Fielding, 2007), although the ligand ideally spans the range of 0.5 K_d to 5 K_d. As it is usually difficult to accurately determine the protein concentration, one can treat the protein concentration as another variable during the fitting procedure, which often leads to significantly improved fits. It is also advised to use many titration curves with 15 to 20 titration points to obtain K_d values as accurate as possible.

Localization of ligand binding sites

Chemical shift mapping

Chemical shift perturbations (CSPs), upon complex formation, are an important source of structural information. The well-known application is the identification of the ligand binding site. Protein residues exhibiting CSP values larger than a defined cut-off are considered as part of the binding site. If the protein ^{15}N-HSQC spectrum is assigned, one can easily identify the binding site by comparing the protein NMR spectra in the bound and free forms. This is illustrated in Figure 17.18.9 for the Peroxiredoxin 5 enzyme (PRDX5) complexed to the 4-methylcatechol. The use of CSPs in drug discovery has been particularly highlighted by the "SAR by NMR" strategy, where two small organic compounds (fragments) binding two adjacent sub-sites are identified by CSP analysis (Shuker et al., 1996). The two fragments are then chemically combined to create a new potent compound.

In the absence of NMR spectrum assignment, the binding site of a molecule can be identified if a known ligand, with a known binding site, is available. CSPs should be observed for a similar series of peaks if the molecule binds the same binding site as the reference ligand. Recently, a method for the rapid identification of ligand-binging sites, using an assignment-free NMR approach, was reported. The approach is based on a cell-free stable isotope labeling procedure that introduces ^{15}N or ^{13}C labels to specific residues of the proteins (Kodama et al., 2013).

J-surface

Considering that the majority of ligands in the pharmaceutical field contain aromatic rings, McCoy and Wyss (2002) have developed a program called *J-surf*, to determinate the position of the ligand aromatic ring center in the binding site. In this approach, they use CSPs to construct a *j-surface*. The principle is that the CSPs observed on the protein NMR spectra are mainly due to the ring current

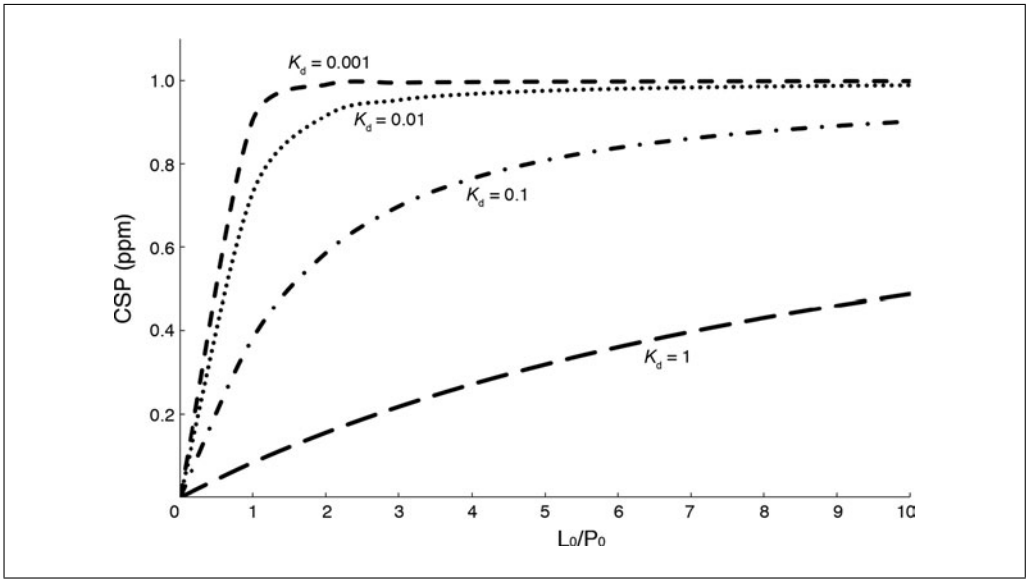

Figure 17.18.8 Theoretical titration curves for the determination of protein-ligand dissociation constant (K_d) by Chemical Shift Perturbation (CSP) measurement. Curves are plotted using $CSP_{max} = 1$ ppm, protein concentration = 100 μM. K_d are given in mM.

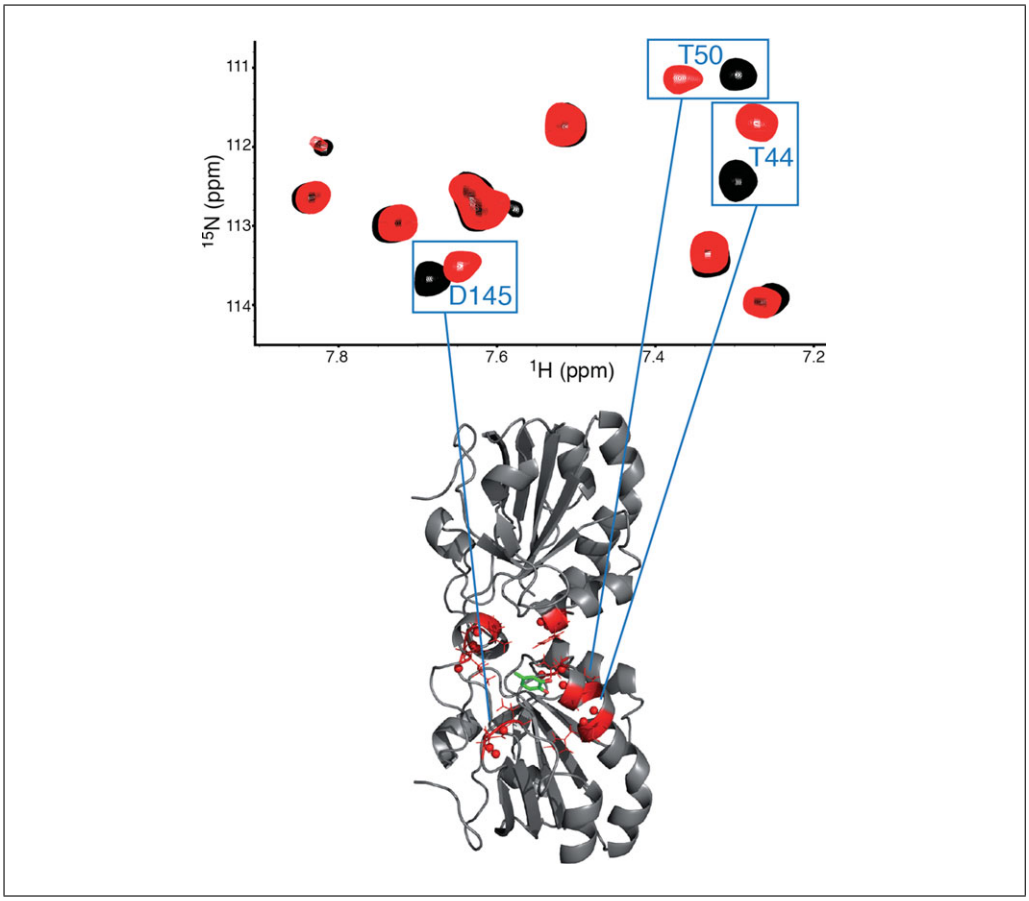

Figure 17.18.9 Identification of the ligand-binding site using Chemical Shift Perturbations (CSPs). The experimental CSPs are mapped on the protein surface. Protein residues exhibiting chemical shift perturbations upon ligand binding are considered as part of the binding site. Spectra are displayed for the free protein (black) and the ligand-bound protein (red).

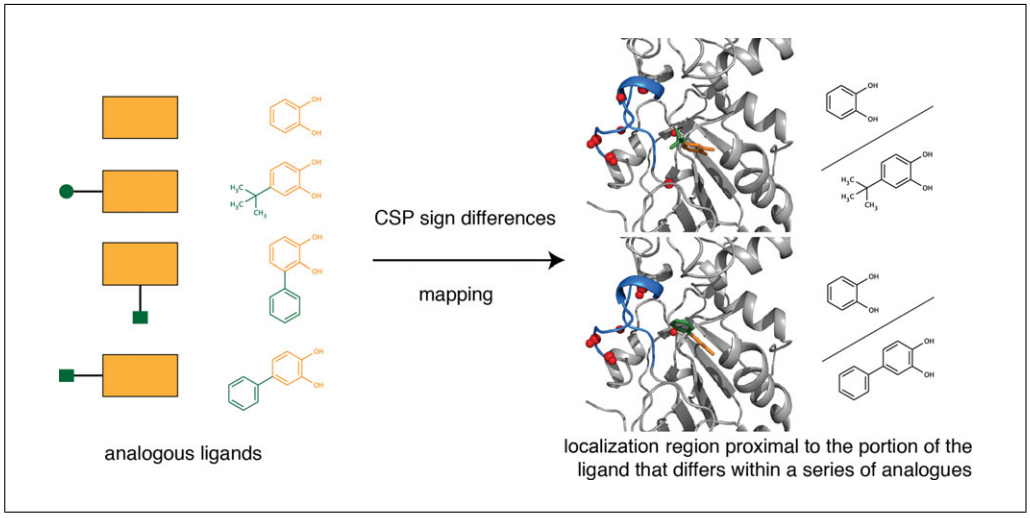

Figure 17.18.10 Binding mode assessment of ligands inferred from the comparative analysis of Chemical Shift Perturbations (CSPs) measured for a series of analogous ligands. CSPs are measured on protein nuclear magnetic resonance (NMR) spectra upon binding. The ligands contain a common core with different substituents (left). The CSP sign differences observed between two analogous ligands are plotted on the protein surface (red spheres) to localize the protein region (blue) proximal to the portion of the ligand that differs within the two ligands (right).

effect of the aromatic rings (Haigh and Mallion, 1979). The *j-surface* is modeled around each perturbed protein proton, and the highest point density of the *j-surface* defines the most likely position of the ligand aromatic ring center. This CSP-based surface can be used for CSP-based 3-D structure determination of protein-ligand complexes, or can be used to check if the CSP data are compatible with a single binding mode of the ligand (Wyss et al., 2004; Cioffi et al., 2008a,b, 2009).

Comparative analysis of analogous ligands

When a series of analogous compounds that bind the same protein target is available, the CSPs induced by these ligands can be compared for assessing the binding site and modes of the ligands in the protein binding site. Medek et al. (2000) first proposed to compare and map, on the protein surface, the CSP magnitude differences induced by the analogous ligands. Using this method, the region of the binding site that is proximal to the portion of the ligand that differs within the series is readily identified, and the ligands may be docked into the binding pocket. The approach was tested for the FKBP-ascomycin complex and Bcl-xL-BAK peptide complex, with CSPs measured on ^{1}H, ^{15}N, or ^{13}C resonances.

In 2008, a new approach was proposed and successfully applied to the MDM2-p53 complex (Riedinger et al., 2008). Here, both the amplitude and the sign (CSP direction) of the CSPs are taken into account to compare the analogous ligands. It was also observed that comparing the magnitude of CSPs induced by analogous ligands could be problematic if the ligands exhibit very different K_d values. In this case, the best method is to compare experimental CSP signs only. This strategy was applied using analogous ligands binding the peroxiredoxin 5 protein target (Aguirre et al., 2014b). Within the series of ligands, the comparison of the shielding and deshielding of each protein amide proton was used to determine if the binding modes of the ligands are conserved or not, depending on the different substituents. It was also possible to determine the protein region toward which the bulky substituents point (Fig. 17.18.10).

Determination of the ligand-binding modes

For the generation of protein-ligand 3-D structures, CSPs can be used as experimental structural constraints in combination with docking programs. In a first approach, CSPs are used as structural information for intermolecular restraints between the protein and the ligand during the structure calculation. In this case, the main information is that a protein residue exhibits (or not) a CSP value, and therefore is located near (or far) from the ligand. In a second more sophisticated approach, both the magnitude and the sign of the protein CSPs are used and compared to CSPs back-calculated using theoretical protein-ligand structures. The experimental protein-ligand structure is the

one that presents the best agreement between experimental and back-calculated CSPs.

CSP as ambiguous intermolecular restrains (AIR) for docking

In the docking program HADDOCK, CSPs can be combined with docking for the generation of protein-ligand 3-D structures (Dominguez et al., 2003). The protein residues exhibiting CSPs larger than a defined cut-off, and located on the protein surface, are identified as "active" residues, while "passive" residues on the protein surface display weaker CSPs than active residues. This approach is used to define the so-called AIR, which represent the restrains between any atom of an active residue on one partner and any atom on all active and passive residues of the second partner.

Schieborr et al. (2005) have developed another docking program, LIGDOCK, which exploits the CSPs in an ambiguous and semi-quantitative fashion (strong, medium, and weak CSPs, with only strong CSPs being used). Here, by contrast with HADDOCK, AIRs are defined unidirectionally from the ligand to the protein. Calculations of the protein-ligand structures are done using the CNS program (Brünger et al., 1998). The solutions are evaluated both with the AIR energy and the CNS energy.

Back-calculation of CSPs

Over the last 15 years, large efforts have been devoted to the prediction of protein chemical shifts, using sequence homology, empirical, semi-classical, and quantum mechanical models (Wishart, 2011). Programs like SHIFTX (Neal et al., 2003; Han et al., 2011), SHIFTS (Xu and Case, 2001; Xu and Case, 2002), SPARTA (Shen and Bax, 2007; Shen and Bax, 2010), and others (Meiler, 2003; Kohlhoff et al., 2009; Lehtivarjo et al., 2009; Sahakyan et al., 2011; Li and Brüschweiler, 2012; Nielsen et al., 2012; Zeng et al., 2013) were developed to back-calculate chemical shifts from the protein 3-D structure. More specifically, chemical shift perturbations (CSPs) induced by a ligand on protein-proton chemical shifts can be back-calculated for virtual protein-ligand structures generated by docking. The comparison of experimental CSPs with simulated CSPs are used for the identification of protein-ligand complex structures in agreement with the experimental data, as discussed in details below.

CSP-based post-docking filter

The pioneering use of CSP back-calculation for the determination of protein-ligand complex structures has been reported by McCoy and Wyss (2000). The method has three main steps: (1) measurement of experimental CSPs induced by the ligand on protein NMR resonances, (2) simulation of CSPs for ligand virtual positions obtained by docking, and (3) comparison of experimental and simulated CSPs to identify the ligand virtual position exhibiting simulated CSPs in best agreement with the experimental NMR data.

McCoy and Wyss have considered that the major contribution of the CSPs, for ligands containing aromatic rings, and in the absence of ligand-induced protein conformational change, is the ring current effect. This ring current effect is simulated using the Haigh-Mallion equation (Equation 17.18.13; Haigh and Mallion, 1979):

$$\mathrm{CSP_{rc}} = fB \sum_{\mathrm{ij}} S_{\mathrm{ij}} \left(\frac{1}{r_{\mathrm{i}}^3} + \frac{1}{r_{\mathrm{j}}^3} \right)$$

Equation 17.18.13

where f is the ring-specific intensity factor (e.g., 1.00 for benzene type ring), B is the nucleus-dependent factor [e.g., $B = 7.06 \times 10^{-6}$ Å for amide protons, or $B = 5.13 \times 10^{-6}$ Å for other protons (Neal et al., 2003)]. The sum is calculated over pairs of bonded ring atoms with ij $\in$ {(1, 2); (2, 3); (3, 4); (4, 5); (5, 6);) (6, 1)}, for a six-membered ring. r_{i} and r_{j} correspond to the distances from the ring atoms i and j to the amide protons of the protein, respectively. S_{ij} is the (algebraic signed) area of the triangle formed by atoms i and j and the target amide proton projected onto the plane of the aromatic ring (here a six-membered ring). As illustrated in Figure 17.18.11, the ring current effect induces a well defined shielding and deshielding effect on protein protons all around the aromatic ring.

McCoy and Wyss used the program SHIFTS for the simulation of CSPs, using aromatic residues as probes to mimic the ring-current effect induced by the ligands, since SHIFTS was developed for the prediction of protein chemical shifts (Wyss et al., 2004; Gorczynski et al., 2007). The CSPs were measured on Hα protons and methionine H*E* protons for the complex between the protein calmodulin and the W-7 ligand (McCoy and Wyss, 2000).

More recently, Cioffi et al. (2008b, 2009) have applied the CSP-based post-docking filter with more sophisticated ligands. A new

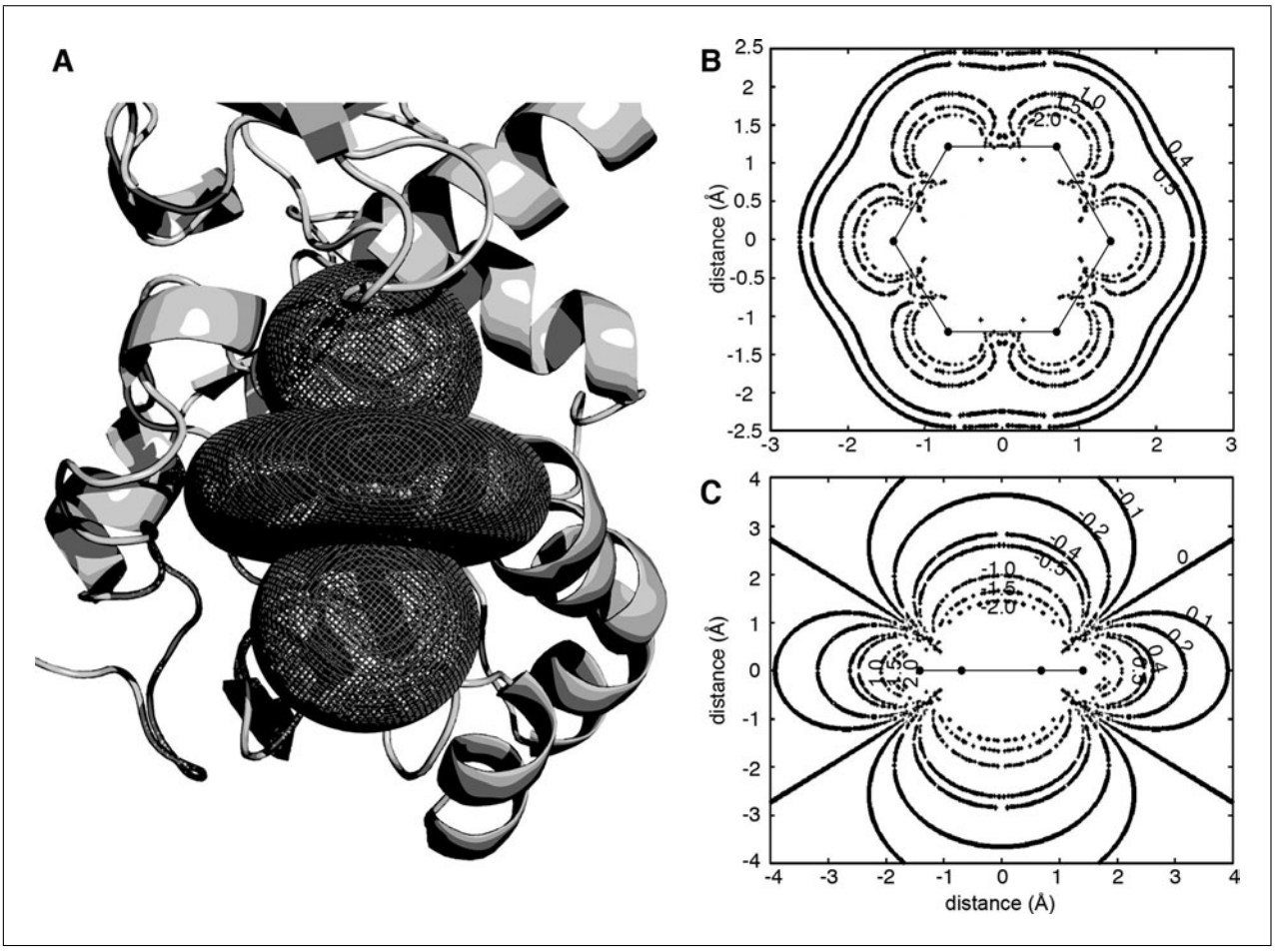

Figure 17.18.11 Ring current effect induced by the aromatic ring of a ligand for the protons of the peroxiredoxin 5 protein. (**A**) Positive (oblate spheroid) and negative (sphere) chemical shift perturbation (CSP) isosurfaces show the theoretical CSP distribution around the ligand aromatic ring. Protein protons localized on the oblate isosurface are affected by a deshielding of +0.7 ppm whereas a proton localized on the sphere isosurface undergoes a deshielding of −0.6 ppm. (**B**) 2-D isosurface plans around the ligand aromatic ring. CSP values are indicated for each curve in the ring plan. (**C**) CSP values are indicated for each curve in a plan perpendicular to the ligand ring.

program Shifty was developed, to allow the authors to back-calculate the CSPs directly with the ligand structures without using amino acids as probes. Three contributions of the CSPs are calculated with Shifty: the ring current effect (Equation (17.18.13), the electric field effect, and the anisotropy effects (Hunter and Packer, 1999). The virtual ligand positions generated by the GOLD docking program were filtered according to the agreement between the simulated and experimental CSPs measured on the protein amide protons.

The electric field was calculated with Equation 17.18.14:

$$\mathrm{CSP_{ef}} = \varepsilon_1 E_z + \varepsilon_2 E^2 = \varepsilon_1 \sum_{\mathrm{i}} \frac{q_{\mathrm{i}} \cos\theta_{\mathrm{i}}}{r_{\mathrm{i}}^2} + \varepsilon_2 \left[\left(\sum_{\mathrm{i}} \frac{q_{\mathrm{i}} \cos\theta_{\mathrm{i}}}{r_{\mathrm{i}}^2} \right)^2 + \left(\sum_{\mathrm{i}} \frac{q_{\mathrm{i}} \sin\theta_{\mathrm{i}}}{r_{\mathrm{i}}^2} \right)^2 \right]$$

Equation 17.18.14

with $\epsilon_1 = -2.0 \times 10^{-12}$ esu and $\epsilon_2 = -1.0 \times 10^{-18}$ esu, r_{i} the distance between atom i and the amide proton, q_{i} the partial charge of atom i, and θ_{i} the angle between the NH vector of the amide group and the HN-i vector,

Finally, the anisotropy effects were simulated as shown in Equation 17.18.15:

$$\mathrm{CSP_{anis}} = \Delta_\chi . \frac{1 - 3\cos^2\theta}{r^3}$$

Equation 17.18.15

with Δ_χ the magnetic susceptibility, r the distance between the protein proton and ligand anisotropic source, and θ the angle between

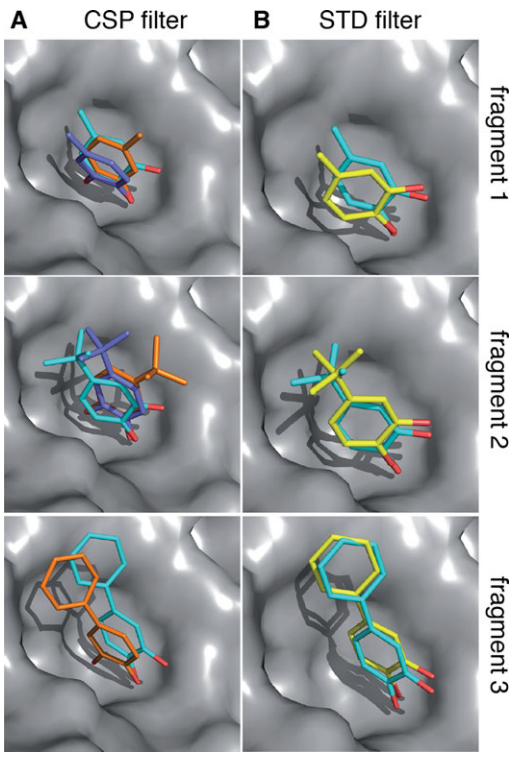

Figure 17.18.12 Determination of the protein-ligand 3-D structure using back-calculated Chemical Shift Perturbations (CSPs) and Saturation Transfer Difference (STD) data for 3 fragment-like ligands, bound to the peroxiredoxin 5 protein. (**A**) Ligand positions selected by CSP simulation from a panel of 200 virtual positions. (**B**) Ligand position in agreement with both the CSP and STD data (cyan), compared to the X-ray structure (yellow).

the *r* vector and the normal of the anisotropic group plane.

To test whether the methodology can be applied to the FBDD strategy, we have back-calculated CSPs for the peroxiredoxin 5 protein complexed with different fragment-like ligands containing aromatic rings (Aguirre et al., 2014b). As shown in Figure 17.18.12, a unique binding mode is not observed. Several binding modes of the fragments are in agreement with the CSP data: the aromatic rings are well positioned with a well defined orientation, but the positions of the substituents are still ambiguous. Therefore, we have suggested adding STD epitope mapping data to better discriminate the correct ligand binding mode from the positions selected by the CSPs. As illustrated in Figure 17.18.12, the complex structures obtained by STD and CSP-based post-docking filter are very close to the X-ray structures.

In 2008, Stark and Powers suggested to include the CSP data in the docking procedure of the AutoDock program (Stark and Powers, 2008). First, CSPs observed for the protein protons allow the location of the ligand-binding site. A restrained volume containing the binding site is defined for the docking, which minimizes the available conformational space for the docking. Then, ligand positions generated by AutoDock4 (Huey et al., 2007) are ranked according to the agreement with the experimental CSPs measured on protein protons. For this step, the authors assume a distance-dependent model between experimental CSPs and the distance between the ligand and the perturbed protein proton, without a back-calculation of the ring current effect.

CSP-guided docking

By contrast with the CSP post-docking filter, where the docked ligand positions are ranked according to their agreement between experimental and simulated CSPs, the CSP-guided docking approach directly includes the back-calculation of CSPs into the scoring function of the docking process. The advantage of this approach is that the results do not depend on the starting positions generated by the docking program. CSP simulation is directly included into the docking process, and an energetic term that maximizes

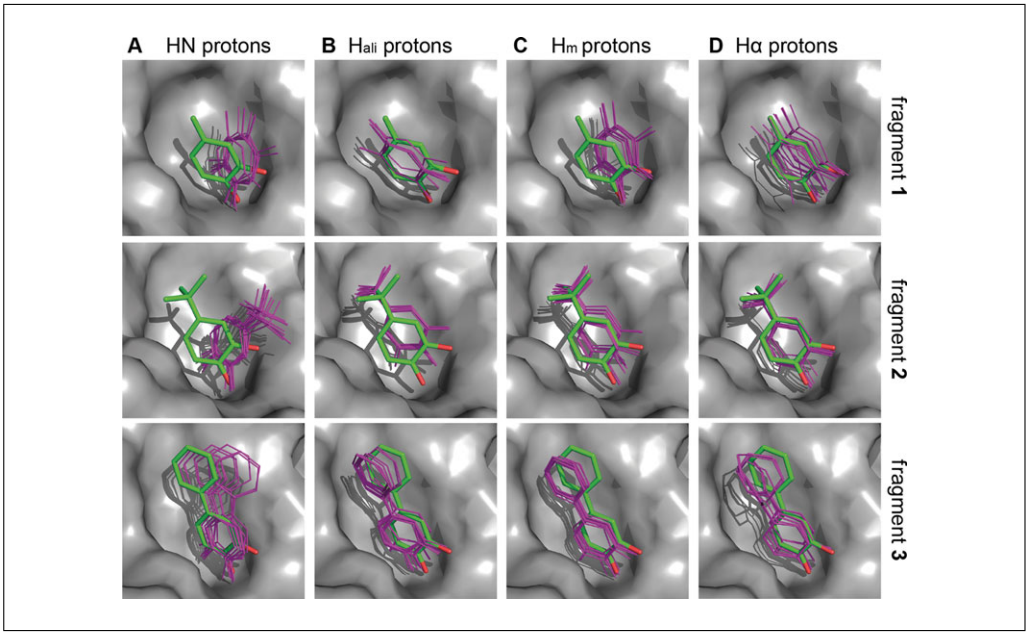

Figure 17.18.13 Ligand binding modes using Chemical Shift Perturbations (CSP)-guided docking, and comparison of the performance of different proton CSPs. The X-ray structures (green) are compared to 10 ligand positions generated by CSP-guided docking with the program PLANTS (purple). Results are given for three analogous fragment-like ligands bound to the peroxiredoxin 5 protein. (**A**) CSPs were measured for amide protons (HN). (**B**) CSPs were measured for aliphatic protons (Hali). (**C**) CSPs were measured for methyl protons (Hm). (**D**) CSPs were measured for α protons (Hα).

the agreement between experimental and simulated data is added to the normal scoring function. Gonzalez-Ruiz and Gohlke (2009) tested the approach with CSPs measured on amide protons.

We have recently modified the PLANTS docking program available for academic research groups (Korb et al., 2007; Korb et al., 2009), to include the CSP simulation in the scoring function. Experimental and simulated CSPs (ring current calculations) were directly included into the docking program PLANTS. We have tested and compared the performance of the CSP-guided docking using different kinds of protein protons (e.g., HN, Hα, Hβ; Aguirre et al., 2014a). As illustrated in Figure 17.18.13, the CSPs measured on Hα protons lead to the best results for the determination of protein-ligand complex structures, while the structures obtained with the amide-proton CSPs displayed the highest Root Mean Square Deviation (RMSD) to the X-ray structures. Finally, CSPs from methyl groups lead to better results than those obtained with the CSPs of amide protons. It is well known that the CSPs of amide protons are very sensitive to conformational changes and in particular to changes in hydrogen bonds (Gonzalez-Ruiz and Gohlke, 2009; Williamson, 2013). These effects are not included in the CSP simulation, which likely explains that the least performing protons for CSP-based docking are the amide proteins. For more details, the reader should see the references (Ten Brink et al., 2014; Aguirre et al., 2014a).

CONCLUSION

In this review, we have given an overview on the most used NMR experiments for the study of protein-ligand interactions. As reported in a large number of publications, NMR can be used for screening compound libraries and the identification of binders, but also for the measurement of the protein-ligand affinities, as well as the characterization of the binding site and binding mode of the ligands. The role of NMR in drug discovery has largely increased during the last decade, and might further evolve in the coming years, in particular for the elaboration of protein-protein inhibitors through the FBDD approach (Valkov et al., 2012; Frank et al., 2013), where NMR appears as one of the best options for such challenging protein-ligand interactions.

ACKNOWLEDGEMENTS

This research was supported by the National Agency of Research in France, ANR grants ANR-11JS07-0008.

LITERATURE CITED

Aguirre, C., ten Brink, T., Cala, O., Guichou, J.-F., and Krimm, I. 2014a. Protein-ligand structure guided by backbone and side-chain proton chemical shift perturbations. *J. Biomol. NMR* 60:147-156.

Aguirre, C., tenBrink, T., Guichou, J.-F., Cala, O., and Krimm, I. 2014b. Comparing binding modes of analogous fragments using NMR in fragment-based drug design: Application to PRDX5. *PLoS One* 9:e102300.

Angulo, J. and Nieto, P.M. 2011. STD-NMR: Application to transient interactions between biomolecules-a quantitative approach. *Eur. Biophys. J.* 40:1357-1369.

Angulo, J., Enríquez-Navas, P.M., and Nieto, P.M. 2010. Ligand-receptor binding affinities from saturation transfer difference (STD) NMR spectroscopy: The binding isotherm of STD initial growth rates. *Chemistry* 16:7803-7812.

Arepalli, S.R., Glaudemans, C.P., Daves, G. Jr., Kovac, P., and Bax, A. 1995. Identification of protein-mediated indirect NOE effects in a disaccharide-Fab' complex by transferred ROESY. *J. Magn. Reson. B* 106:195-198.

Barelier, S., Pons, J., Gehring, K., Lancelin, J.-M., and Krimm, I. 2010. Ligand specificity in fragment-based drug design. *J. Med. Chem.* 53:5256-5266.

Bartoschek, S., Klabunde, T., Defossa, E., Dietrich, V., Stengelin, S., Griesinger, C., Carlomagno, T., Focken, I., and Wendt, K.U. 2010. Drug design for G-protein-coupled receptors by a ligand-based NMR method. *Angew. Chem. Int. Ed. Engl.* 49:1426-1429.

Basilio, N., Martn-Pastor, M., and Garca-Ro, L. 2012. Insights into the structure of the supramolecular amphiphile formed by a sulfonated calix[6]arene and alkyltrimethylammonium surfactants. *Langmuir* 28:6561-6568.

Becattini, B., Culmsee, C., Leone, M., Zhai, D., Zhang, X., Crowell, K.J., Rega, M.F., Landshamer, S., Reed, J.C., Plesnila, N., and Pellecchia, M. 2006. Structure-activity relationships by interligand NOE-based design and synthesis of antiapoptotic compounds targeting Bid. *Proc. Natl. Acad. Sci. U.S.A.* 103:12602-12606.

Begley, D.W., Zheng, S., and Varani, G. 2010. Fragment-based discovery of novel thymidylate synthase leads by NMR screening and group epitope mapping. *Chem. Biol. Drug Des.* 76:218-233.

Benie, A.J., Moser, R., Bäuml, E., Blaas, D., and Peters, T. 2003. Virus-ligand interactions: Identification and characterization of ligand binding by NMR spectroscopy. *J. Am. Chem. Soc.* 125:14-15.

Bhunia, A., Bhattacharjya, S., and Chatterjee, S. 2012. Applications of saturation transfer difference NMR in biological systems. *Drug Discov. Today* 17:505-513.

Breukels, V., Konijnenberg, A., Nabuurs, S.M., Doreleijers, J.F., Kovalevskaya, N.V., and Vuister, G.W. 2011. Overview on the use of NMR to examine protein structure. *Curr. Protoc. Protein Sci.* 64:17.5.1-17.5.44.

Brünger, A.T., Adams, P.D., Clore, G.M., DeLano, W.L., Gros, P., Grosse-Kunstleve, R.W., Jiang, J.-S., Kuszewski, J., Nilges, M., Pannu, N.S., Read, R.J., Rice, L.M., Simonson, T., and Warren, G.L. 1998. Crystallography & NMR system: A new software suite for macromolecular structure determination. *Acta Crystallogr. D Biol. Crystallogr.* 54:905-921.

Cala, O., Guillière, F., and Krimm, I. 2014. NMR-based analysis of protein-ligand interactions. *Anal. Bioanal. Chem.* 406:943-956.

Campos-Olivas, R. 2011. NMR screening and hit validation in fragment based drug discovery. *Curr. Top. Med. Chem.* 11:43-67.

Carlomagno, T. 2012. NMR in natural products: Understanding conformation, configuration and receptor interactions. *Nat. Prod. Rep.* 29:536-554.

Chen, J., Zhang, Z., Stebbins, J.L., Zhang, X., Hoffman, R., Moore, A., and Pellecchia, M. 2007. A fragment-based approach for the discovery of isoform-specific p38alpha inhibitors. *ACS Chem. Biol.* 2:329-336.

Cioffi, M., Hunter, C.A., and Packer, M.J. 2008a. Influence of conformational flexibility on complexation-induced changes in chemical shift in a neocarzinostatin protein-ligand complex. *J. Med. Chem.* 51:4488-4495.

Cioffi, M., Hunter, C.A., Packer, M.J., and Spitaleri, A. 2008b. Determination of protein ligand binding modes using complexation-induced changes in ^{1}H NMR chemical shift. *J. Med. Chem.* 51:2512-2517.

Cioffi, M., Hunter, C.A., Packer, M.J., Pandya, M.J., and Williamson, M.P. 2009. Use of quantitative ^{1}H NMR chemical shift changes for ligand docking into barnase. *J. Biomol. NMR* 43:11-19.

Claasen, B., Axmann, M., Meinecke, R., and Meyer, B. 2005. Direct observation of ligand binding to membrane proteins in living cells by a saturation transfer double difference (STDD) NMR spectroscopy method shows a significantly higher affinity of integrin αIIbβ3 in native platelets than in liposomes. *J. Am. Chem. Soc.* 127:916-919.

Dalvit, C., Cottens, S., Ramage, P., and Hommel, U. 1999. Half-filter experiments for assignment, structure determination and hydration analysis of unlabelled ligands bound to 13C/15N labelled proteins. *J. Biomol. NMR* 13:43-50.

Dalvit, C., Fogliatto, G., Stewart, A., Veronesi, M., and Stockman, B. 2001. WaterLOGSY as a method for primary NMR screening: Practical aspects and range of applicability. *J. Biomol. NMR* 21:349-359.

Dalvit, C., Pevarello, P., Tatò, M., Veronesi, M., Vulpetti, A., and Sundström, M. 2000a. Identification of compounds with binding affinity to proteins via magnetization transfer from bulk water. *J. Biomol. NMR* 18:65-68.

Dalvit, C., Pevarello, P., Tat, M., Veronesi, M., Vulpetti, A., and Sundstrm, M. 2000b.

Identification of compounds with binding affinity to proteins via magnetization transfer from bulk water. *J. Biomol. NMR* 18:65-68.

Dalvit, C., Fasolini, M., Flocco, M., Knapp, S., Pevarello, P., and Veronesi, M. 2002. NMR-based screening with competition water-ligand observed via gradient spectroscopy experiments: Detection of high-affinity ligands. *J. Med. Chem.* 45:2610-2614.

DiMicco, J.A. and Zaretsky, D.V. 2005. The mysterious role of prostaglandin E2 in the medullary raphé: A hot topic or not? *Am. J. Physiol. Regul. Integr. Comp. Physiol.* 289:R1589-R1591.

Dominguez, C., Boelens, R., and Bonvin, A.M.J.J. 2003. HADDOCK: A protein-protein docking approach based on biochemical or biophysical information. *J. Am. Chem. Soc.* 125:1731-1737.

Erlanson, D.A. 2012. Introduction to fragment-based drug discovery. *Top. Curr. Chem.* 317:1-32.

Fielding, L. 2007. NMR methods for the determination of protein-ligand dissociation constants. *Prog. Nucl. Magn. Res. Spectr.* 51:219-242.

Frank, A.O., Feldkamp, M.D., Kennedy, J.P., Waterson, A.G., Pelz, N.F., Patrone, J.D., Vangamudi, B., Camper, D.V., Rossanese, O.W., Chazin, W.J., and Fesik, S.W. 2013. Discovery of a potent inhibitor of replication protein a protein-protein interactions using a fragment-linking approach. *J. Med. Chem.* 56:9242-9250.

Goldflam, M., Tarragó, T., Gairí, M., and Giralt, E. 2012. NMR studies of protein-ligand interactions. *Methods Mol. Biol.* 831:233-259.

Gonzalez-Ruiz, D. and Gohlke, H. 2009. Steering protein-ligand docking with quantitative NMR chemical shift perturbations. *J. Chem. Inf. Model.* 49:2260-2271.

Gorczynski, M.J., Grembecka, J., Zhou, Y., Kong, Y., Roudaia, L., Douvas, M.G., Newman, M., Bielnicka, I., Baber, G., Corpora, T., Shi, J., Sridharan, M., Lilien, R., Donald, B.R., Speck, N.A., Brown, M.L., and Bushweller, J.H. 2007. Allosteric inhibition of the protein-protein interaction between the leukemia-associated proteins Runx1 and CBFβ. *Chem. Biol.* 14:1186-1197.

Haigh, C.W. and Mallion, R.B. 1979. Ring current theories in nuclear magnetic resonance. *Prog. Nucl. Magn. Reson. Spectrosc.* 13:303-344.

Han, B., Liu, Y., Ginzinger, S.W., and Wishart, D.S. 2011. SHIFTX2: Significantly improved protein chemical shift prediction. *J. Biomol. NMR* 50:43-57.

Harner, M.J., Frank, A.O., and Fesik, S.W. 2013. Fragment-based drug discovery using NMR spectroscopy. *J. Biomol. NMR* 56:65-75.

Huey, R., Morris, G.M., Olson, A.J., and Goodsell, D.S. 2007. A semiempirical free energy force field with charge-based desolvation. *J. Comput. Chem.* 28:1145-1152.

Hunter, C.A. and Packer, M.J. 1999. Complexation-induced changes in ^{1}H NMR chemical shift for supramolecular structure determination. *Chem. Eur. J.* 5:1891-1897.

Jayalakshmi, V. and Krishna, N.R. 2002. Complete relaxation and conformational exchange matrix (CORCEMA) analysis of intermolecular saturation transfer effects in reversibly forming ligand-receptor complexes. *J. Magn. Reson.* 155:106-118.

Kodama, Y., Takeuchi, K., Shimba, N., Ishikawa, K., ichiro Suzuki, E., Shimada, I., and Takahashi, H. 2013. Rapid identification of ligand-binding sites by using an assignment free NMR approach. *J. Med. Chem.* 56:9342-9350.

Kohlhoff, K.J., Robustelli, P., Cavalli, A., Salvatella, X., and Vendruscolo, M. 2009. Fast and accurate predictions of protein NMR chemical shifts from interatomic distances. *J. Am. Chem. Soc.* 131:13894-13895.

Korb, O., Stützle, T., and Exner, T.E. 2007. An ant colony optimization approach to flexible protein-ligand docking. *Swarm Intelligence* 2:115-134.

Korb, O., Stützle, T., and Exner, T.E. 2009. Empirical scoring functions for advanced protein-ligand docking with PLANTS. *J. Chem. Inf. Model.* 49:84-96.

Krimm, I. 2012. INPHARMA-based identification of ligand binding site in fragment-based drug design. *MedChemComm* 5:605-610.

Krimm, I., Lancelin, J.-M., and Praly, J.-P. 2012. Binding evaluation of fragment-based scaffolds for probing allosteric enzymes. *J. Med. Chem.* 55:1287-1295.

Lehtivarjo, J., Hassinen, T., Korhonen, S.-P., Peräkylä, M., and Laatikainen, R. 2009. 4D prediction of protein ^{1}H chemical shifts. *J. Biomol. NMR* 45:413-426.

Li, D.-W. and Brüschweiler, R. 2012. PPM: A side-chain and backbone chemical shift predictor for the assessment of protein conformational ensembles. *J. Biomol. NMR* 54:257-265.

Li, D., DeRose, E.F., and London, R.E. 1999. The inter-ligand Overhauser effect: A powerful new NMR approach for mapping structural relationships of macromolecular ligands. *J. Biomol. NMR* 15:71-76.

Ludwig, C. and Guenther, U.L. 2009. Ligand based NMR methods for drug discovery. *Front. Biosci. (Landmark Ed.)* 14:4565-4574.

Ludwig, C., Michiels, P.J.A., Wu, X., Kavanagh, K.L., Pilka, E., Jansson, A., Oppermann, U., and Gnther, U.L. 2008. SALMON: Solvent accessibility, ligand binding, and mapping of ligand orientation by NMR spectroscopy. *J. Med. Chem.* 51:1-3.

Mari, S., Serrano-Gómez, D., Cañada, F.J., Corbí, A.L., and Jiménez-Barbero, J. 2005. 1D saturation transfer difference NMR experiments on living cells: The DCSIGN/oligomannose interaction. *Angew. Chem. Int. Ed. Engl.* 44:296-298.

Maurer, T. 2005. NMR studies of protein-ligand interactions. *Methods Mol. Biol.* 305:197-214.

Mayer, M. and James, T.L. 2004. NMR-based characterization of phenothiazines as a RNA binding scaffold. *J. Am. Chem. Soc.* 126:4453-4460.

Mayer, M. and Meyer, B. 1999. Characterization of ligand binding by saturation transfer difference NMR spectroscopy. *Angew. Chem. Int. Ed. Engl.* 38:1784-1788.

Mayer, M. and Meyer, B. 2001. Group epitope mapping by saturation transfer difference NMR to identify segments of a ligand in direct contact with a protein receptor. *J. Am. Chem. Soc.* 123:6108-6117.

McCoy, M.A. and Wyss, D.F. 2000. Alignment of weakly interacting molecules to protein surfaces using simulations of chemical shift perturbations. *J. Biomol. NMR* 18:189-198.

McCoy, M.A. and Wyss, D.F. 2002. Spatial localization of ligand binding sites from electron current density surfaces calculated from NMR chemical shift perturbations. *J. Am. Chem. Soc.* 124:11758-11763.

McCoy, M.A., Senior, M.M., and Wyss, D.F. 2005. Screening of protein kinases by ATP-STD NMR spectroscopy. *J. Am. Chem. Soc.* 127:7978-7979.

Medek, A., Hajduk, P.J., Mack, J., and Fesik, S.W. 2000. The use of differential chemical shifts for determining the binding site location and orientation of protein-bound ligands. *J. Am. Chem. Soc.* 122:1241-1242.

Meiler, J .2003. PROSHIFT: Protein chemical shift prediction using artificial neural networks. *J. Biomol. NMR* 26:25-37.

Meinecke, R. and Meyer, B. 2001. Determination of the binding specificity of an integral membrane protein by saturation transfer difference NMR: RGD peptide ligands binding to integrin αIIbβ3. *J. Med. Chem.* 44:3059-3065.

Meyer, B. and Peters, T. 2003. NMR spectroscopy techniques for screening and identifying ligand binding to protein receptors. *Angew. Chem. Int. Ed. Engl.* 42:864-890.

Mooij, W.T. M., Hartshorn, M.J., Tickle, I.J., Sharff, A.J., Verdonk, M.L., and Jhoti, H. 2006. Automated protein-ligand crystallography for structure-based drug design. *ChemMedChem* 1:827-838.

Moseley, H.N., Curto, E.V., and Krishna, N.R. 1995. Complete relaxation and conformational exchange matrix (CORCEMA) analysis of NOESY spectra of interacting systems; two-dimensional transferred NOESY. *J. Magn. Reson. B* 108:243-261.

Murray, C.W., Erlanson, D.A., Hopkins, A.L., Keserü, G.M., Leeson, P.D., Rees, D.C., Reynolds, C.H., and Richmond, N.J. 2014. Validity of ligand efficiency metrics. *ACS Med. Chem. Lett.* 5:616-618.

Nagaraja, C. 2006. Heteronuclear saturation transfer difference (HSTD) experiment for detection of ligand binding to proteins. *Chem. Phys. Lett.* 420:340-346.

Neal, S., Nip, A.M., Zhang, H., and Wishart, D.S. 2003. Rapid and accurate calculation of protein ^{1}H, ^{13}C and ^{15}N chemical shifts. *J. Biomol. NMR* 26:215-240.

Nielsen, J.T., Eghbalnia, H.R., and Nielsen, N.C. 2012. Chemical shift prediction for protein structure calculation and quality assessment using an optimally parameterized force field. *Prog. Nucl. Magn. Reson. Spectrosc.* 60:1-28.

Ono, K., Takeuchi, K., Ueda, H., Morita, Y., Tanimura, R., Shimada, I., and Takahashi, H. 2014. Structure-based approach to improve a small-molecule inhibitor by the use of a competitive peptide ligand. *Angew. Chem. Int. Ed. Engl.* 53:2597-2601.

Orts, J., Griesinger, C., and Carlomagno, T. 2009. The INPHARMA technique for pharmacophore mapping: A theoretical guide to the method. *J. Magn. Reson.* 200:64-73.

Pereira, A., Pfeifer, T.A., Grigliatti, T.A., and Andersen, R.J. 2009. Functional cell-based screening and saturation transfer double-difference NMR have identified haplosamate A as a cannabinoid receptor agonist. *Chem. Biol.* 4:139-144.

Post, C.B. 2003. Exchange-transferred noe spectroscopy and bound ligand structure determination. *Curr. Opin. Struct. Biol.* 13:581-588.

Rademacher, C., Krishna, N.R., Palcic, M., Parra, F., and Peters, T. 2008. NMR experiments reveal the molecular basis of receptor recognition by a calicivirus. *J. Am. Chem. Soc.* 130:3669-3675.

Rademacher, C., Guiard, J., Kitov, P.I., Fiege, B., Dalton, K.P., Parra, F., Bundle, D.R., and Peters, T. 2011. Targeting norovirus infection-multivalent entry inhibitor design based on NMR experiments. *Chemistry* 17:7442-7453.

Räuber, C. and Berger, S. 2010. 13C-NMR detection of STD spectra. *Magn. Reson. Chem.* 48:91-93.

Ravindranathan, S., Mallet, J.-M., Sinay, P., and Bodenhausen, G. 2003. Transferred cross-relaxation and cross-correlation in NMR: Effects of intermediate exchange on the determination of the conformation of bound ligands. *J. Magn. Reson.* 163:199-207.

Reese, M., Snchez-Pedregal, V.M., Kubicek, K., Meiler, J., Blommers, M.J. J., Griesinger, C., and Carlomagno, T. 2007. Structural basis of the activity of the microtubule-stabilizing agent epothilone a studied by NMR spectroscopy in solution. *Angew. Chem. Int. Ed. Engl.* 46:1864-1868.

Rega, M.F., Wu, B., Wei, J., Zhang, Z., Cellitti, J.F., and Pellecchia, M. 2011. SAR by interligand nuclear overhauser effects (ILOEs) based discovery of acylsulfonamide compounds active against Bcl-x(L) and Mcl-1. *J. Med. Chem.* 54:6000-6013.

Riedinger, C., Endicott, J.A., Kemp, S.J., Smyth, L.A., Watson, A., Valeur, E., Golding, B.T., Griffin, R.J., Hardcastle, I.R., Noble, M.E., and McDonnell, J.M. 2008. Analysis of chemical shift changes reveals the binding modes of isoindolinone inhibitors of the MDM2 p53 interaction. *J. Am. Chem. Soc.* 130:16038-16044.

Sahakyan, A.B., Vranken, W.F., Cavalli, A., and Vendruscolo, M. 2011. Structure-based

prediction of methyl chemical shifts in proteins. *J. Biomol. NMR* 50:331-346.

Sánchez-Pedregal, V.M., Reese, M., Meiler, J., Blommers, M.J. J., Griesinger, C., and Carlomagno, T. 2005. The INPHARMA method: Protein-mediated interligand NOEs for pharmacophore mapping. *Angew. Chem. Int. Ed. Engl.* 44:4172-4175.

Schieborr, U., Vogtherr, M., Elshorst, B., Betz, M., Grimme, S., Pescatore, B., Langer, T., Saxena, K., and Schwalbe, H. 2005. How much NMR data is required to determine a protein-ligand complex structure? *Chembiochem* 6:1891-1898.

Shen, Y. and Bax, A. 2007. Protein backbone chemical shifts predicted from searching a database for torsion angle and sequence homology. *J. Biomol. NMR* 38:289-302.

Shen, Y. and Bax, A. 2010. SPARTA+: A modest improvement in empirical NMR chemical shift prediction by means of an artificial neural network. *J. Biomol. NMR* 48:13-22.

Shuker, S.B., Hajduk, P.J., Meadows, R.P., and Fesik, S.W. 1996. Discovering high-affinity ligands for proteins: SAR by NMR. *Science* 274:1531-1534.

Siebert, H.-C., Lü, S.-Y., Frank, M., Kramer, J., Wechselberger, R., Joosten, J., André, S., Rittenhouse-Olson, K., Roy, R., von der Lieth, C.-W., Kaptein, R., Vliegenthart, J.F. G., Heck, A.J. R., and Gabius, H.-J. 2002. Analysis of protein-carbohydrate interaction at the lower size limit of the protein part (15-mer peptide) by NMR spectroscopy, electrospray ionization mass spectrometry, and molecular modeling. *Biochemistry* 41:9707-9717.

Sledz, P., Silvestre, H.L., Hung, A.W., Ciulli, A., Blundell, T.L., and Abell, C. 2010. Optimization of the interligand Overhauser effect for fragment linking: Application to inhibitor discovery against *Mycobacterium tuberculosis* pantothenate synthetase. *J. Am. Chem. Soc.* 132:4544-4545.

Sousa, S.F., Ribeiro, A.J. M., Coimbra, J.T. S., Neves, R.P. P., Martins, S.A., Moorthy, N.S. H.N., Fernandes, P.A., and Ramos, M.J. 2013. Protein-ligand docking in the new millennium—a retrospective of 10 years in the field. *Curr. Med. Chem.* 20:2296-2314.

Stark, J. and Powers, R. 2008. Rapid protein-ligand costructures using chemical shift perturbations. *J. Am. Chem. Soc.* 130:535-545.

Szczepina, M.G., Bleile, D.W., and Pinto, B.M. 2011. Investigation of the binding of a carbohydrate-mimetic peptide to its complementary anticarbohydrate antibody by STD NMR spectroscopy and molecular-dynamics simulations. *Chemistry* 17:11446-11455.

Szczepina, M.G., Zheng, R.B., Completo, G.C., Lowary, T.L., and Pinto, B.M. 2009. STD-NMR studies suggest that two acceptor substrates for GlfT2, a bifunctional galactofuranosyltransferase required for the biosynthesis of *Mycobacterium tuberculosis* arabinogalactan, compete for the same binding site. *Chembiochem* 10:2052-2059.

Ten Brink, T., Aguirre, C., Exner, T.E., and Krimm, I. 2014. Performance of protein-ligand docking with simulated chemical shift perturbations. *J. Chem. Inf. Model.* 55:275-283.

Valkov, E., Sharpe, T., Marsh, M., Greive, S., and Hyvönen, M. 2012. Targeting protein-protein interactions and fragment-based drug discovery. *Top. Curr. Chem.* 317:145-179.

Wagstaff, J.L., Taylor, S.L., and Howard, M.J. 2013. Recent developments and applications of saturation transfer difference nuclear magnetic resonance (STD NMR) spectroscopy. *Mol. Biosyst.* 9:571-577.

Wang, Y.-S., Liu, D., and Wyss, D.F. 2004. Competition STD NMR for the detection of high-affinity ligands and NMR-based screening. *Magn. Res. Chem.*42:485-489.

Williamson, M.P. 2013. Using chemical shift perturbation to characterise ligand binding. *Prog. Nucl. Magn. Reson. Spectrosc.* 73:1-16.

Wishart, D.S. 2011. Interpreting protein chemical shift data. *Prog. Nucl. Magn. Reson. Spectrosc.* 58:62-87.

Wyss, D.F., Arasappan, A., Senior, M.M., Wang, Y.-S., Beyer, B.M., Njoroge, F.G., and McCoy, M.A. 2004. Non-peptidic small-molecule inhibitors of the single-chain hepatitis C virus NS3 protease/NS4A cofactor complex discovered by structure-based NMR screening. *J. Med. Chem.* 47:2486-2498.

Xu, X.P. and Case, D.A. 2001. Automated prediction of $^{13}C\beta$ and $^{13}C'$ chemical shifts in proteins using a density functional database. *J. Biomol. NMR* 21:321-333.

Xu, X.-P. and Case, D.A. 2002. Probing multiple effects on ^{15}N, $^{13}C\alpha$, $^{13}C\beta$, and $^{13}C'$ chemical shifts in peptides using density functional theory. *Biopolymers* 65:408-423.

Yuan, Y., Wen, X., Sanders, D.A. R., and Pinto, B.M. 2005. Exploring the mechanism of binding of UDP-galactopyranose to UDP-galactopyranose mutase by STD-NMR spectroscopy and molecular modeling. *Biochemistry* 44:14080-14089.

Zeng, J., Zhou, P., and Donald, B.R. 2013. HASH: A program to accurately predict protein Hα shifts from neighboring backbone shifts. *J. Biomol. NMR* 55:105-118.